Aalborg Universitet

AALBORG UNIVERSITY
DENMARK

Modelling of Natural and Hybrid Ventilation

Heiselberg, Per Kvols

Publication date:
2006

Document Version
Accepted author manuscript, peer reviewed version

Link to publication from Aalborg University

Citation for published version (APA):
Heiselberg, P. (2006). Modelling of Natural and Hybrid Ventilation. Aalborg: Department of Civil Engineering, Aalborg University. DCE Lecture notes, No. 4

General rights
Copyright and moral rights for the publications made accessible in the public portal are retained by the authors and/or other copyright owners and it is a condition of accessing publications that users recognise and abide by the legal requirements associated with these rights.

? Users may download and print one copy of any publication from the public portal for the purpose of private study or research.
? You may not further distribute the material or use it for any profit-making activity or commercial gain
? You may freely distribute the URL identifying the publication in the public portal ?

Take down policy
If you believe that this document breaches copyright please contact us at vbn@aub.aau.dk providing details, and we will remove access to the work immediately and investigate your claim.

Downloaded from vbn.aau.dk on: January 17, 2019

Modelling of Natural and Hybrid Ventilation

Per Heiselberg

ISSN 1901-7286
DCE Lecture Notes No. 004

AALBORG UNIVERSITY
Department of Civil Engineering

Aalborg University
Department of Civil Engineering
Indoor Environmental Engineering

DCE Lecture Notes No. 004

Modelling of Natural and Hybrid Ventilation

by

Per Heiselberg

December 2006

© Aalborg University

Scientific Publications at the Department of Civil Engineering

Technical Reports are published for timely dissemination of research results and scientific work carried out at the Department of Civil Engineering (DCE) at Aalborg University. This medium allows publication of more detailed explanations and results than typically allowed in scientific journals.

Technical Memoranda are produced to enable the preliminary dissemination of scientific work by the personnel of the DCE where such release is deemed to be appropriate. Documents of this kind may be incomplete or temporary versions of papers—or part of continuing work. This should be kept in mind when references are given to publications of this kind.

Contract Reports are produced to report scientific work carried out under contract. Publications of this kind contain confidential matter and are reserved for the sponsors and the DCE. Therefore, Contract Reports are generally not available for public circulation.

Lecture Notes contain material produced by the lecturers at the DCE for educational purposes. This may be scientific notes, lecture books, example problems or manuals for laboratory work, or computer programs developed at the DCE.

Theses are monograms or collections of papers published to report the scientific work carried out at the DCE to obtain a degree as either PhD or Doctor of Technology. The thesis is publicly available after the defence of the degree.

Latest News is published to enable rapid communication of information about scientific work carried out at the DCE. This includes the status of research projects, developments in the laboratories, information about collaborative work and recent research results.

Published 2006 by
Aalborg University
Department of Civil Engineering
Sohngaardsholmsvej 57,
DK-9000 Aalborg, Denmark

Printed in Denmark at Aalborg University

ISSN 1901-7286
DCE Lecture Notes No. 004

CONTENTS

1 INTRODUCTION

The effectiveness of natural ventilation, i.e. its ability to ensure indoor air quality and passive cooling in a building, depends greatly on the design process. Mechanical ventilation systems can be designed separately from the design of the building in which they are installed. They can also be installed in existing buildings after a few modifications. In contrast, ventilation systems using only natural forces such as wind and thermal buoyancy need to be designed together with the building, since the building itself and its components are the elements that can reduce or increase air movement as well as influence the air content (dust, pollution etc.). Architects and engineers need to acquire qualitative and quantitative information about the interactions between building characteristics and natural ventilation in order to design buildings and systems consistent with a passive low-energy approach.

Natural ventilation can be used to provide fresh air for the occupants, necessary to maintain acceptable air quality levels, and to cool buildings in cases where the climatic conditions allow it. Natural ventilation is caused by pressure differences at the inlets and outlets of a building envelope, as a result of wind velocity and/or stack effect. Natural ventilation can be achieved by infiltration and/or by allowing air to flow in and out of a building by opening windows and doors.

The term infiltration is used to describe the random flow of outdoor air through leakage paths in the building's envelope. The presence of cracks and a variety of unintentional openings, their sizes and distribution determine the leakage characteristics of a building and its potential for air infiltration. Modern architecture tends to minimize air infiltration by introducing "air-tight" buildings, where the cracks in the structure are sealed. Infiltration rates vary seasonally in response to outdoor temperature and wind conditions. Infiltration associated air-change rates may vary from a low of 0.1-0.2 air changes pr hour in tight, energy efficient houses to 2-3 air changes per hour (ACH) in leaky houses under high-infiltration conditions, while, with the windows wide open during summer, it is possible to achieve 15-20 ACH. Even larger air changes, around 30 ACH, can be achieved by natural means, but there is a need for large number of window openings and careful placement within the space. It is important to link the necessary number of windows and their placement with the requirements for natural lighting purposes.

The effectiveness of natural ventilation is determined by the prevailing outdoor conditions – microclimate (wind speed, temperature, humidity and surrounding topography) and the building itself (orientation, number of windows or openings, size and location). In addition to the use of windows and other openings for natural ventilation, there are some additional means of enhancing the air movement. Wind towers utilise the kinetic energy of wind, which is properly channelled within the building in order to generate air movement within a space. They have been successfully integrated in many architectural designs. Solar chimneys are constructions used to promote air movement throughout the building using solar gains. They are positioned on the sunward side of the building to make the best possible use of direct solar gains.

Natural ventilation is used to create a volumetric flow, for renewal of indoor air and transfer of heat, resulting from the outdoor wind speed and/or stack effects in order to remove heat stored into the building materials and to enhance heat dissipation from the human body to the environment. The savings from natural ventilation depend on the number of air changes, the construction of the building (heavy or light construction), the microclimate and the temperature and humidity in the space.

Outdoor temperature, humidity and wind velocity are determinant factors for the successful application of natural ventilation techniques. For cooling purposes, the incoming air should be at a lower temperature that the indoor air temperature. However, even at higher temperatures, the resulting air flow inside the space can cause a positive effect on the thermal comfort conditions of the occupants, since it increases heat dissipation from the human body end enhances evaporative and convective heat losses. Natural ventilation techniques for cooling purposes are also very effective during the night hours, when outdoor air temperatures are usually lower than the indoor ones. As a result the cooling load is reduced and the peak indoor air temperatures can be reduced by 1 to 3 °C.

Air humidity is the most important limiting factor for the application of natural ventilation techniques. High levels of humidity have a negative influence on thermal comfort. As a result, in regions with high relative humidity levels during summer, the use of conventional air-conditioning systems is necessary in order to remove water vapour from indoor air. Under such circumstances, natural ventilation during the day- or night-time hours should be avoided.

Hybrid ventilation systems can be described as systems that provide a comfortable internal environment using both natural ventilation and mechanical systems, but using different features of these systems at different times of the day or season of the year. In hybrid ventilation mechanical and natural forces are combined in a two-mode system where the operating mode varies according to the season, and within individual days. Thus the active mode reflects the external environment and takes maximum advantage of ambient conditions at any point in time. The main difference between a conventional ventilation system and a hybrid system is the fact that the latter has an intelligent control system that can switch automatically between natural and mechanical modes in order to minimize energy consumption.

There are multiple motivations for the interest in hybrid ventilation. The most obvious are:

- Hybrid ventilation has access to both ventilation modes in one system, exploits the benefits of each mode and creates new opportunities for further optimisation and improvement of the overall quality of ventilation.
- Advanced hybrid ventilation technology fulfils the high requirements on indoor environmental performance and the increasing need for energy savings and sustainable development by optimising the balance between indoor air quality, thermal comfort, energy use and environmental impact.
- Hybrid ventilation results in high user satisfaction because of the use of natural ventilation, the high degree of individual control of the indoor climate

(including the possibility of varying the indoor climate - adaptive comfort) as well as a direct and visible response to user interventions.

- Hybrid ventilation technology offers an intelligent and advanced ventilation solution for the complex building developments of today, that is user transparent and sustainable.

Naturally, expectations of hybrid ventilation performance will vary between different countries because of climate variations, energy prices and other factors. In countries with cold climates, hybrid ventilation can avoid the trend to use mechanical air conditioning in new buildings, which has occurred in response to higher occupant expectations, the requirements of codes and standards, and in some cases higher internal gains and changes in building design. In countries with warm climates, it can reduce the reliance on air conditioning and reduce the cost, energy penalty and consequential environmental effects of full year-round air conditioning.

Both natural and mechanical ventilation have advantages and disadvantages. For natural ventilation systems one of the major disadvantages is the uncertainty in performance, which results in an increased risk of draught problems and/or low indoor air quality in cold climates and a risk of unacceptable thermal comfort conditions during summer periods. On the other hand, air conditioning systems often lead to complaints from the occupants, especially in cases where individual control is not possible. Hybrid ventilation systems have access to both ventilation modes and therefore allow the best ventilation mode to be chosen depending on the circumstances.

The focus on the environmental impacts of energy production and consumption has provided an increased awareness of the energy used by fans, heating/cooling coils and other equipment in ventilation and air conditioning systems. An expectation of a reduction in annual energy costs has also been an important driving force for the development of hybrid ventilation strategies. Available data from case studies provided in the international project IEA ECBCS-Annex 35 (Heiselberg 2002) show that a substantial energy saving has been achieved in a number of buildings, mainly because of a very substantial reduction in energy use for fans and a reduced energy use for cooling.

Buildings with natural ventilation are associated with less SBS-symptoms, than buildings with traditional ventilation systems, (Seppänen and Fisk, 2002). Natural ventilation is well accepted by occupants and the natural ventilation mode should therefore be used, when the climatic conditions allow it. In addition the high degree of user control in hybrid ventilation systems has an influence on the perceived indoor environmental quality. Another aspect is that hybrid ventilation implies less noise (provided that there are no outdoor sources of heavy noise), which may also improve the perceived quality. In ECBCS-Annex 35 the high degree of user control in the investigated buildings was greatly appreciated by the occupants. In one of the cases (Rowe 2002) investigations via occupant questionnaires showed that the perceived performance increased as a function of perceived indoor air quality and thermal comfort.

Estimating the initial cost of hybrid ventilation systems in buildings can be quite difficult as the installation often consists of both mechanical installations and of building elements. Part of the investment in mechanical equipment is often shifted

towards a larger investment in the building itself: increased room air volume per person, a shape favourable to air movement, a more intelligent facade/window system, etc. On the other hand the building might provide more useable (rentable) space, as space for plant rooms, stacks for ventilation channels, etc., is not needed. Recently a method for calculation of Life Cycle Costs (LCC) of natural ventilation systems have been developed, (Vik, 2003), which takes all these issues into consideration. This method can as well be applied on buildings with hybrid ventilation systems.

In ECBCS-Annex 35 the reference cost range provided by the participants was used to compare the initial costs of hybrid ventilation systems, and buildings with hybrid ventilation, with the initial cost of traditional systems and buildings, see (van der Aa, 2002). The life cycle costs for hybrid ventilated buildings were often lower than for reference buildings, but the relationship between initial, operating and maintenance costs was different.

These lecture notes focus on modelling of natural and hybrid ventilation driven by thermal buoyancy, wind and/or mechanical driving forces for a single zone with one, two or several openings.

1.1 Natural driving forces

1.1.1 Thermal Buoyancy

Natural ventilation by thermal buoyancy is the air exchange between two or more zones with different air densities due to difference in temperatures and/or moisture content, where the last effect usually is of minor importance. Ventilation by air exchange implies openings between the zones and the opening arrangement can either be separate small openings in different levels or it can be a single large vertical or horizontal opening. The temperature difference can occur due to heating one or more of the zones. After a while steady-state conditions will exist with a balance between the heat supply, the temperature difference, the resulting ventilation capacity and the heat losses. It is this steady-state situation that is dealt with in the following

When there is no wind the external and internal pressure distribution can be described by:

$$P = P_0 - \rho_0 g H \qquad \text{(Eq. 1.1.1)}$$

where P is the external or internal pressure [Pa]
P_0 is the pressure at a reference level (floor) [Pa]
ρ_0 is the external or internal air density at a reference level [kg/m^3]
g is gravitational acceleration [m/s^2]
H is height above the reference level [m]

For the external air, P_0 is determined by conditions in the atmosphere. For the internal air, if the space were sealed P_0 could take any value depending on the mass of the enclosed air and its volume and temperature as given by the perfect gas law. When there are openings in the envelope the value of P_0 under steady equilibrium conditions is still determined by the mass of the contained air, but this mass is governed by a relationship between the internal pressure and the flow rate through the openings.

Applying (Eq. 1.1.1) to the external and internal air gives the following expression for the pressure difference Δp across an opening at the height z:

$$\Delta p_t = P_{u0} - P_{i0} - gz(\rho_u - \rho_i) \qquad \text{(Eq. 1.1.2)}$$

When temperature differences are not large (<30K) and the air can be regarded as imcompressible, the temperature and density differences are approximately related by (from the equation of state):

$$\frac{\rho_u - \rho_i}{\rho_i} \cong \frac{T_i - T_u}{T_u} \qquad \text{(Eq. 1.1.3)}$$

where ρ_u is the external air density [kg/m^3]
ρ_i is the internal air density [kg/m^3]
T_u is external temperature [K]
T_i is internal temperature [K]

The position of the neutral height above the floor, H_o, is given by putting $\Delta p = 0$, which gives the pressure difference between the zones at the reference level (floor) as:

$$P_{u0} - P_{i0} = \rho_i g H_o \frac{T_i - T_u}{T_u} \qquad \text{(Eq. 1.1.4)}$$

The pressure difference for an opening at height H_1 becomes:

$$\Delta p_1 = P_{u0} - P_{i0} - \rho_i g H_1 \frac{T_i - T_u}{T_u} \qquad \text{(Eq. 1.1.5)}$$

$$\Delta p_1 = \rho_i g H_o \frac{T_i - T_u}{T_u} - \rho_i g H_1 \frac{T_i - T_u}{T_u} = \rho_i g \frac{T_i - T_u}{T_u}(H_o - H_1) \qquad \text{(Eq. 1.1.6)}$$

It is seen that for openings below the neutral plane the pressure difference is positive and for openings above the neutral plane the pressure difference is negative.

Example 1

For a 20m high building with a top and a bottom opening and a temperature difference of 20°C between indoor and outdoor (indoor temperature is 22 °C) the maximum pressure difference by thermal buoyancy across one of the openings will be:

$$\Delta p_t = \rho_i g \frac{T_i - T_u}{T_u}\left(H_o - H_1\right) = 1{,}20 \cdot 9{,}82 \frac{20}{285}(10) = 8{,}3Pa$$

Figure 1 shows how the maximum pressure difference due to thermal buoyancy across one of the openings in the building depends on the buildings height and the indoor-outdoor temperature difference. It is seen that the pressure differences are quite small, especially for buildings with only one story.

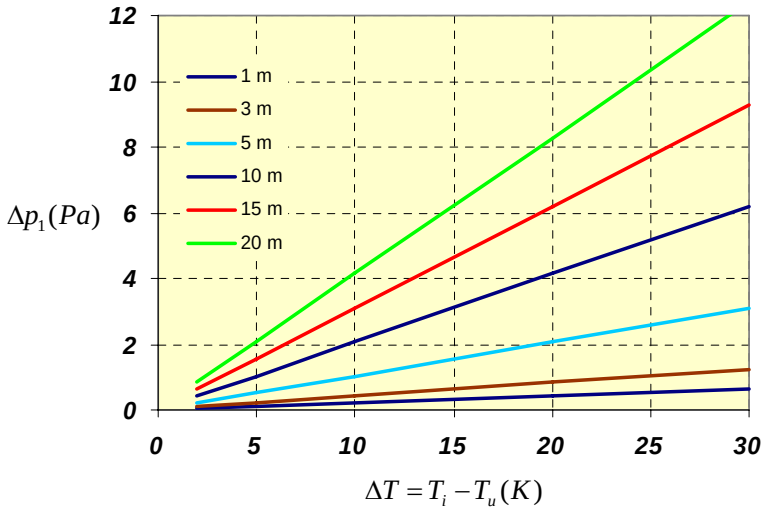

Figure 1. For a building with a bottom and a top opening the maximum pressure difference due to thermal buoyancy across one of the openings is shown as a function of building height and temperature difference.

1.1.2 Wind pressure

Natural ventilation by wind is the air exchange between two or more zones because of wind-induced pressure differences on the building facades that propagate into the interior of the building. On the windward side of a building there will be an over pressure and on the other sides, there will be under pressure. If the slope of the roof is not too high there will also be under pressure on the roof. With increasing slope of the roof there will be an over pressure on the windward side of the roof on a larger and larger area starting from the bottom parts. Ventilation by air exchange implies openings between the zones and the opening arrangement can either be on opposite sides of the building (cross ventilation) or it can be a single large vertical or horizontal opening. In the last situation the air exchange will be driven by differences in wind pressures in the opening and wind fluctuations.

The pressure due to wind flow into or away from a surface is proportional to the dynamic pressure and is given by:

$$P_w = C_p \tfrac{1}{2} \rho_u v_{ref}^2 \qquad \text{(Eq. 1.1.7)}$$

where P_w is wind induced pressure [Pa]
C_p is pressure coefficient [-]
ρ_u is external air density [kg/m^3]
v_{ref} is wind speed at a reference height (usually building height) [m/s]

The dimensionless pressure coefficient C_p is an empirically derived parameter that accounts for the changes in wind-induced pressure, caused by the influence of surrounding obstructions on the prevailing local wind characteristics. Its value changes according to the wind direction, the building surface orientation and the topography and roughness of the terrain in the wind direction. Typical design data sets based on experimental results are given in Table 1. Every data set comprises C_p values for 16 different wind directions (angle of the wind with the normal to the surface: 0°, 22.5°, 45°, 67.5° 90°, 112.5°, 135°, 157.5°, 180°, 202.5° 225°, 247.5°, 270°, 292.5°, 315°, 337.5°, progressing clockwise as seen from above). Table 1 comprises 29 pressure coefficient data sets corresponding to an equal number of different facade configurations in terms of surface aspect, dimensions and exposure. The C_p values may be used for low-rise buildings of up to three storeys and they express an average value for each external building surface.

Table 1. Pressure coefficient sets. /Santamouris/.

No.	Facade description	AR*	Exp†	Cp sets
1	Wall	1:1	E	0.7, 0.525, 0.35, −0.075, −0.5, −0.45, −0.4, −0.3, −0.2, −0.3, −4, −0.45, −0.5, −0.075, 0.35, 0.525
2	Roof, pitch > 10°	1:1	E	−0.8, −0.75, −0.7, −0.65, −0.6, −0.55, −0.5, −0.45, −0.4, -0.45, −0.5, −0.55, −0.6, −0.65, −0.7, −0.75
3	Roof, pitch > 10–30°	1:1	E	−0.4, −0.45, −0.5, −0.55, −0.6, −0.55, −0.5, −0.45, −0.4, −0.45, −0.5, −0.55, −0.6, −0.55, −0.5, −0.45
4	Roof, pitch > 30°	1:1	E	−0.3, −0.35, −0.4, −0.5, −0.6, −0.5, −0.4, −0.45, −0.5, −0.45,−0.4, −0.5, −0.6, −0.5, −0.4, −0.35
5	Wall	1:1	SE	0.4, 0.25, 0.1, −0.1, −0.3, −0.325, −0.35, 0.275, −0.2, −0.275, −0.35, −0.325, −0.3, −0.1, 0.1, 0.25
6	Roof, pitch < 10°	1:1	SE	−0.6, −0.55, −0.5, −0.45, −,4, −0.45, −0.5, −0.55, −0.6, − 0.55, −0.5, −0.45, −0.4, −0.45, −0.5, −0.55
7	Roof, pitch 10–30°	1:1	SE	−0.35, −0.4, −0.45, −0.5, −0.55, −0.5, −0.45, −0.4, −0.35, −0.4, −0.45, −0.5, −0.55, −0.5, −0.45, −0.4
8	Roof. pitch > 30°	1:1	SE	−0.3. −0.4, −0.5, −0.55, −0.6, −0.55, −0.5, −0.5, −0.5, −0.5, −0.5, −0.55, −0.6, −0.55, −0.5, −0.4
9	Wall	1:1	S	0.2, 0.125, 0.05, 0.1, −0.25, −0.275, −0.3, −0.275, −0.25, −0.275, −0.3, −0.275, −0.25, −0.1, 0.05, 0.125
10	Roof, pitch < 10 deg	1:1	S	−0.5, −0.5, −0.5, −0.45, −0.4, −0.45, −0.5, −0.5, −0.5, −0.5, −0.5, −0.45, −0.4, −0.45, −0.5, −0.5
11	Roof, pitch 10–30°	1:1	S	−0.3, −0.35, −0.4, −0.45, −0.5, −0.45, −0.4, −0.35, −0.3, −0.35, −0.4, −0.45, −0.5, −0.45, −0.4, −0.35
12	Roof, pitch > 30°	1:1	S	0.25, −0.025, −0.3, −0.4, −0.5, −0.4, −0.3, −0.35, −0.4, −0.35, −0.3, −0.4, −0.5, −0.4, −0.3, −0.025
13	Long wall	2:1	E	0.5, 0.375, 0.25, −0.125, −0.5, −0.65, −0.8, −0.75, −0.7, −0.75, −0.8, −0.65, −0.5, −0.125, −0.25, −0.375
14	Short wall	1:2	E	−0.9, −0.35, 0.2, 0.4, 0.6, 0.4, 0.2, −0.35, −0.9, −0.75, −0.6, −0.475, −0.35, −0.475, −0.6, −0.75
15	Roof, pitch < 10°	2:1	E	−0.7, −0.7, −0.7, −0.75, −0.8, −0.75, −0.7, −0.7, −0.7, −0.7, −0.7, −0.75, −0.8, −0.75, −0.7, −0.7
16	Roof, pitch 10–30°	2:1	E	−0.7, −0.7, −0.7, −0.7, −0.7, −0.65, −0.6, −0.55, −0.5, −0.55, −0.6, −0.65, −0.7, −0.7, −7, −0.7
17	Roof, pitch > 30°	2:1	E	0.25. 0.125. 0. −0.3. −0.6. −0.75. −0.9. −0.85. −0.8. −0.85, −0.9, −0.75, −0.6, −0.3, 0, 0.125
18	Long Wall	2:1	SE	0.5, 0.375, 0.25, 0.−125, −0.5, −0.65, −0.8, −0.75, −0.7, −0.75, −0.8, −0.65, −0.5, −0.125, 0.25, 0.375
19	Short Wall	1:2	SE	−0.9, −0.35, 0.2, 0.4, 0.6, 0.4, 0.2, −0.35, −0.9, −0.75, −0.6, −0.475, −0.35, −0.475, −0.6, −0.75
20	Roof, pitch < 10°	2:1	SE	−0.7, −0.7, −0.7, −0.75, −0.8, −0.75, −0.7, −0.7, −0.7, −0.7, −0.7, −0.75, −0.8, −0.75, −0.7, −0.7
21	Roof, pitch 10–30°	2:1	SE	−0.7, −0.7, −0.7, −0.7, −0.7, −0.65, −0.6, −0.55. −0.5. −0.55, −0.6, −0.65, −0.7, −0.7, −0.7, −0.7
22	Roof, pitch > 30°	2:1	SE	0.25, 0.125, 0, −0.3, −0.6, −0.75, −0.9, −0.85, −0.8, −0.85, −0.9, −0.75, −0.6, −0.3, 0, 0.125
23	Long wall	2:1	S	0.06, −0.03, −0.12, −0.16, −0.2, −0.29, −0.38, −0.34, −0.3, −0.34, −0.38, −0.29, −0.2, −0.16, −0.12, −0.03
24	Short wall	1:2	S	−0.3, −0.075, 0.15, 0.165, 0.18, 0.165, 0.15, −0.075, −0.3, −0.31, −0.32, −0.32, −0.26, −0.2, −0.26, −0.32
25	Roof, pitch < 10°	2:1	S	−0.49, −0.475, −0.46, −0.435, −0.41, −0.435, −0.46, −0.475, −0.49, −0.475, −0.46, −0.435, −0.41, −0.435, −0.46, −0.475
26	Roof, pitch 10–30°	2:1	S	−0.49, −0.475, −0.46, −0.435, −0.41, −0.435, −0.46, −0.43, −0.4, −0.43, −0.46, −0.435, −0.41, −0.435, −0.46, −0.475
27	Roof, pitch > 30°	2:1	S	0.06, −0.045, −0.15, −0.19, −0.23, −0.42, −0.6, −0.51, −0.42, −0.51, −0.6, −0.42, −0.23, −0.19, −0.15, −0.045
28	Wall	1:1	E	0.9, 0.7, 0.5, 0.2, −0.1, −0.1, −0.2, −0.2, −0.2, −0.2, −0.2, −0.1, −0.1, 0.2, 0.5, 0.7
29	Roof, no pitch	1:1	E	−0.1, −0.1, −0.1, −0.1, −0.1 −0.1 −0.1 −0.1, −0.1, −0.1, −0.1, −0.1, −0.1, −0.1, −0.1, −0.1

*AR aspect ratio (length-to-width ratio) † Exp exposure: E exposed; SE Semi-exposed; S Sheltered

Local (not wall averaged) evaluation of the C_p parameter is one of the most difficult aspects of natural ventilation modelling. Figure 2 shows the distribution of C_p values on a building for different wind directions.

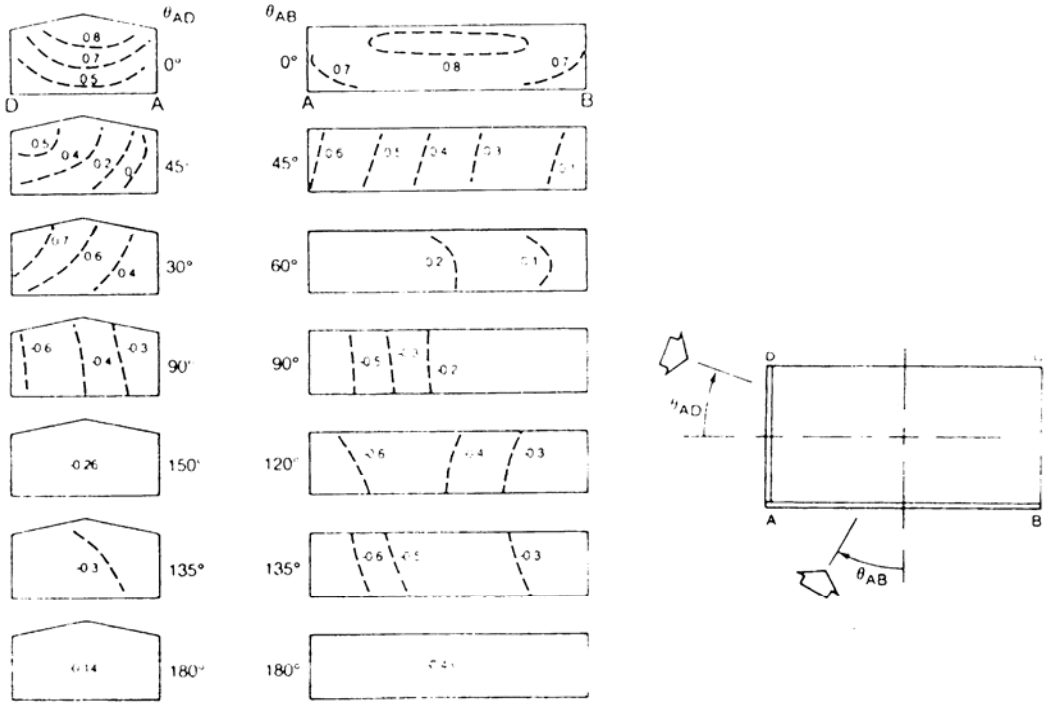

Figure 2. Example of the distribution of C_p on a building. /Allard/.

The form of the roof of a building affects the wind pressure distribution on the roof and on the upper parts of the facades. Consequently the air flow beneath the roof, through attic spaces and rooms located on the upper floor, is modified. A flat roof, a single-slope roof with a pitch up to 15° or a single-slope roof facing downwind has negative pressures over all the surface at any angle of the oncoming wind. Above 15° pitch, when the wind angle is perpendicular to the eaves line, the pressure becomes positive

- At a tilt angle of about 15°, in the middle of the slope
- At a tilt angle of about 25°, also on the area near the ridge
- At a tilt angle of about 35° over all the surface of the slope

Both slopes of a double-slope roof are under negative pressure over all their surfaces up to a pitch of 21°, regardless of wind direction. The leeward slope of a double-slope roof is always under negative pressure, regardless of roof pitch. On the windward slope, with wind perpendicular to the eaves line pressures becomes positive

- At a pitch of about 21°, in the middle of the slope
- At a pitch of about 33°, also near the eaves

Near the ridge, pressure is positive for pitches of between 30° and 41° and negative above 41°.

When the angle of incidence of the wind is 30° to the normal to the eaves line, the windward slope of a double-slope roof is under positive pressure: above a pitch of 22°, in the middle of the slope, and above a pitch of 30°, also near the eaves. Near the ridge, pressure is positive for pitches of between 35° and 50° and negative above 50°. When the angle of incidence of the wind is 60° to the normal to the eaves line, the windward slope of a double-slope roof is under positive pressure in the middle of the slope and

near to the eaves, above a pitch of 30°. The area near to the ridge is under negative pressure up to pitches of over 50°.

The pressure difference across an opening can be calculated as:

$$\Delta p_w = P_w - P_i \quad \Leftrightarrow \quad \Delta p_w = \tfrac{1}{2} C_p \rho_u v_{ref}^2 - P_i \qquad \text{(Eq. 1.1.8)}$$

where P_i is the internal pressure in the building [Pa]

The pressure difference across a building can be calculated as:

$$\Delta p_w = \tfrac{1}{2} C_{p,w} \rho_u v_{ref}^2 - \tfrac{1}{2} C_{p,l} \rho_u v_{ref}^2 = \Delta C_p \tfrac{1}{2} \rho_u v_{rej}^2 \qquad \text{(Eq. 1.1.9)}$$

Example 2

Wind flow perpendicular on one side of a square building with flat roof creates a surface pressure level on the windward side of building proportional to a pressure coefficient of C_p = 0,7 and on the roof proportional to a pressure coefficient of C_p = -0,8. For a reference wind velocity of v_{ref} = 9 m/s, the wind pressure difference will be:

$$\Delta p_w = \Delta C_p \tfrac{1}{2} \rho_u v_{rej}^2 = \left(0.7 - \left(-0.8\right)\right) \cdot 0.5 \cdot 1.2 \cdot \left(9\right)^2 = 72.9 Pa$$

Figure 3 shows the pressure difference created by wind between different building surfaces as a function of reference wind speed. It is seen that the pressure differences are much higher than for thermal buoyancy and are very dependent on which surfaces openings are located.

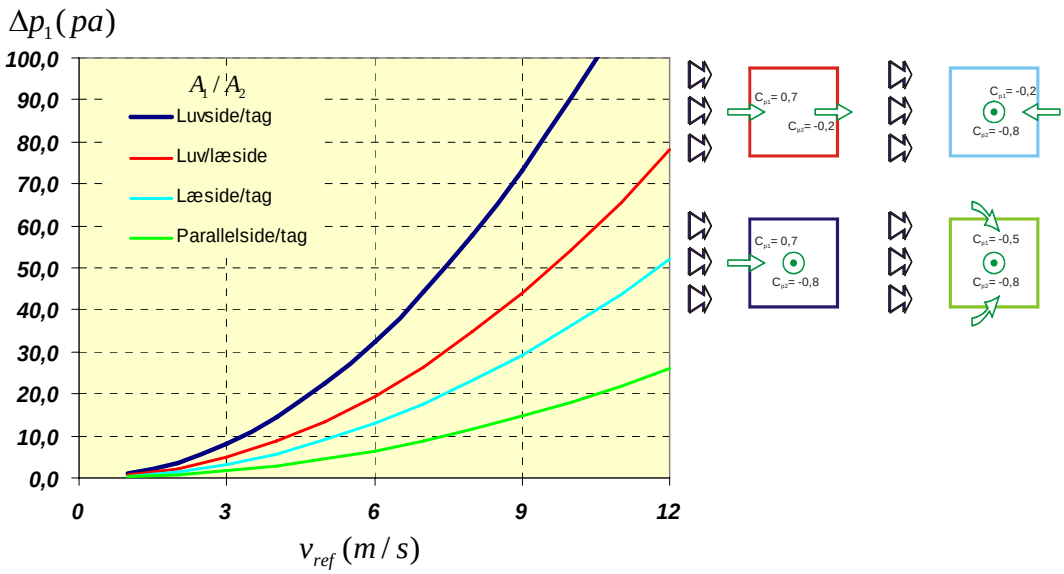

Figure 3.Example of pressure difference created by wind between different building surfaces as a function of reference wind speed.

1.1.3 Combined thermal buoyancy and wind pressure

In practice the natural driving forces will almost always be acting together. The total driving forces are found as the sum of the driving forces. From Eq. 1.1.6 and Eq. 1.1.8 we get:

$$\Delta p = \Delta p_w + \Delta p_t = ½ C_p \rho_u v_{ref}^2 - P_i + \frac{\rho_u \Delta T}{T_i} g(H_0 - H) \qquad \text{(Eq. 1.1.10)}$$

1.2 Mechanical driving forces

In hybrid systems the natural driving forces can be assisted by mechanical fans. The relationship between pressure difference and air flow through a fan must be modelled in order to include the performance in modelling of hybrid systems.

Measured pressure-flow data for operating fans are often given as base fan performance curves. These can be approximated by the following parabolic equation:

$$\Delta p_{m,o} = a_0 + a_1 q_{m,o} + a_2 q_{m,o}^2 \qquad \text{(Eq. 1.2.1)}$$

where $q_{m,o}$ is the air flow rate at a reference rotational speed and fan size [m^3/s]

$\Delta p_{m,o}$ is the pressure difference at a reference rotational speed and fan size [Pa]

a_0, a_1, a_2 are empirically determined coefficients

The properties of fans operating are often only specified at a limited number of conditions but by using the fan laws it is possible to model the performance of geometrical similar fans at different rotational speeds.

The fan laws provide the following approximate relations between air flow rate, pressure difference, rotational speed and fan size:

$$\frac{q_m}{q_{m,o}} = \frac{n}{n_o}\left(\frac{D}{D_o}\right)^3 \qquad \frac{\Delta p_m}{\Delta p_{m,o}} = \left(\frac{n}{n_o}\right)^2 \left(\frac{D}{D_o}\right)^2 \qquad \text{(Eq. 1.2.2)}$$

where q_m is the air flow rate at the actual rotational speed and fan size [m^3/s]

Δp_m is the pressure difference at the actual rotational speed and fan size [Pa]

n, n_o are the actual and the reference rotational speed, respectively [r/min]

D, D_o are the actual and the reference fan size, respectively [-]

A fan performance curve can be derived for geometrical similar fans at different rotational speeds:

$$\Delta p_m = a_0 \left(\frac{n}{n_o}\right)^2 \left(\frac{D}{D_o}\right)^2 + a_1 q_m \left(\frac{n}{n_o}\right)\left(\frac{D}{D_o}\right)^{-1} + a_2 q_m^2 \left(\frac{D}{D_o}\right)^{-4} \qquad \text{(Eq. 1.2.3)}$$

Example 3

For an axial fan operating at a rotational speed of 600 rpm the following relation between pressure and flow applies:

$q_{m,o}$ [m^3/s]	0.000	0.054	0.109	0.170	0.221	0.272	0.331	0.433	0.500	0.556	0.605
$\Delta p_{m,o}$ [Pa]	85	70	60	50	40	30	20	10	0	-10	-20

The coefficients a_o, a_1 and a_2 in Eq. 1.2.3 can be obtained by regression by using the method of least

squares. Using the data in the above table the following values are obtained: a_o = 82.525, a_1 = -205.587 and a_2 = 68.829. To predict the performance for other rotational speeds Eq. 1.2.5 can be used:

$$\Delta p_m = 82.525\left(\frac{n}{600}\right)^2 - 205.587 q_m\left(\frac{n}{600}\right) + 68.829 q_m^2$$

Figure 4 shows the modelled fan performance for different rotational speeds (including 0 rpm) together with pressure flow data given in the tables.

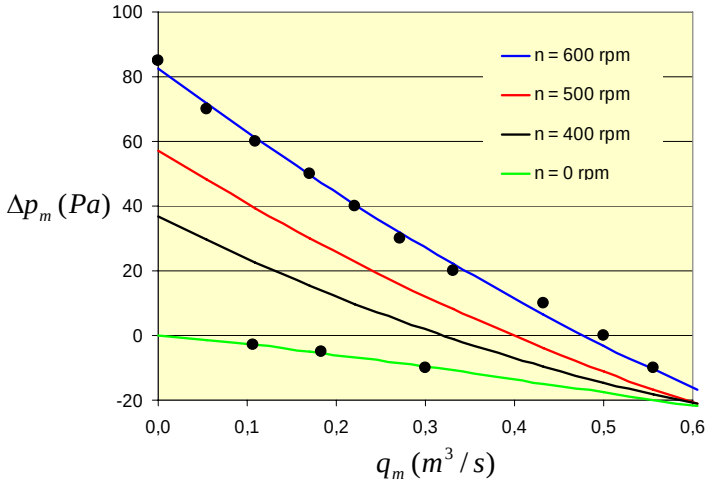

Figure 4. Modelled fan performance for different rotational speeds compared with given pressure flow data.

1.3 Flow through envelope openings

Unidirectional air flow through openings in the building envelope will take shape of a jet. The jet will have the smallest cross section, the so-called vena contracta, shortly after the opening. In vena contracta the air pressure is equal to the surrounding pressure, because the streamlines are parallel and therefore the pressure gradient to the flow direction is zero. Besides the air velocity can be considered as uniform.

The air velocity in the vena contracta can be related to the pressure difference between inside and outside across the opening by imagining a stream line between an arbitrary outside point (point 1 in Figure 5) and a point in vena contracta. Along this streamline the modified Bernouilli equation (taking the friction into account) is valid. The friction loss is often given as a pressure drop, Δp_{fr}, and the following equation is given for the inlet:

$$p_i + \tfrac{1}{2}\rho_o v_c^2 = p_3 + g\rho_o y_3 - \Delta p_{fr} = p_o - \Delta p_{fr} \qquad \text{(Eq. 1.3.1)}$$

where
- P_i is the internal pressure in centre of opening [Pa]
- P_o is the external pressure in centre of opening [Pa]
- P_3 is the external pressure in point 3 [Pa]
- ρ_0 is the external air density [kg/m^3]
- v_c is the velocity in vena contracta [m/s]
- g is gravitational acceleration [m/s^2]

y_3 is height above the centre of the opening [m]
ΔP_{fr} is the pressure drop due to friction loss [Pa]

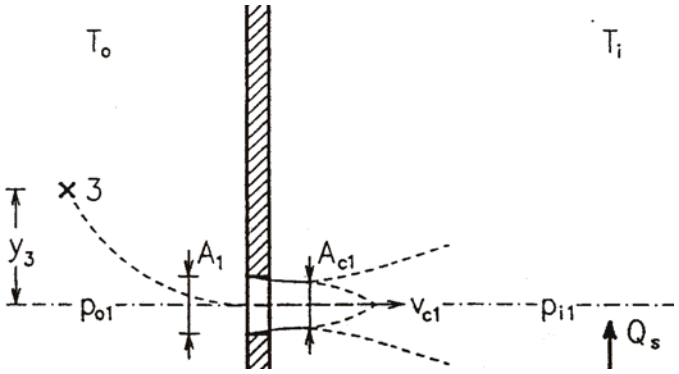

Figure 5. Air flow through an envelope opening.

Eq. 1.3.1 can be written as:

$$½\rho_o v_c^2 = (p_o - p_i) - \Delta p_{fr} \qquad \text{(Eq. 1.3.2)}$$

or

$$v_c = \sqrt{\frac{2(p_o - p_i)}{\rho_o}\left(1 - \frac{\Delta p_{fr}}{(p_o - p_i)}\right)} \qquad \text{(Eq. 1.3.3)}$$

The velocity coefficient can be defined by:

$$v_c = C_v v_{theo} = C_v \sqrt{\frac{2(p_o - p_i)}{\rho_o}} \qquad \text{(Eq. 1.3.4)}$$

where v_{theo} is the theoretical obtainable velocity with no friction loss [m/s]
C_v is the velocity coefficient [-]

From Eq. 1.3.3 and 1.3.4 we find the velocity coefficient to be:

$$C_v = \sqrt{\left(1 - \frac{\Delta p_{fr}}{(p_o - p_i)}\right)} \qquad \text{(Eq. 1.3.5)}$$

The friction loss for the flow through a short opening (short in the flow direction) is small compared to the loss in a pipe. The ratio $\Delta p_{fr}/\Delta p$ will have a value of 0,02 – 0,1. Estimating a value of 0.1 will be on the safe side, and it gives:

$$C_v = \sqrt{(1 - 0.1)} = 0.95 \qquad \text{(Eq. 1.3.6)}$$

The friction loss can also be expressed through the so-called resistance coefficient defined by:

$$\Delta p_{fr} = \varsigma \tfrac{1}{2} \rho_o v_c^2 \qquad \text{(Eq. 1.3.7)}$$

The modified Bernouilli equation (taking the friction into account) then becomes:

$$p_i + \tfrac{1}{2} \rho_o v_c^2 + \varsigma \tfrac{1}{2} \rho_o v_c^2 = p_3 + g \rho_o y_3 = p_o \qquad \text{(Eq. 1.3.8)}$$

The velocity in vena contracta becomes:

$$v_c = \sqrt{\frac{2(p_o - p_i)}{\rho_o}\left(\frac{1}{(1+\varsigma)}\right)} \qquad \text{(Eq. 1.3.9)}$$

and

$$C_v = \sqrt{\frac{1}{1+\varsigma}} \qquad \text{(Eq. 1.3.10)}$$

The air flow rate through the envelope opening is calculated by:

$$q = A_c v_c = C_c A C_v v_{theo} = C_d A v_{theo} \qquad \text{(Eq. 1.3.11)}$$

where q is the air flow rate [m^3/s]
A_c is the area of vena contracta [m^2]
C_c is the contraction coefficient [-]
C_d is the discharge coefficient [-]

The discharge coefficient is defined as the ratio between the real and the theoretical flow rate:

$$C_d = \frac{q_{real}}{q_{theo}} = \frac{C_c A C_v v_{theo}}{A v_{theo}} = C_v C_c \qquad \text{(Eq. 1.3.12)}$$

The value of the contraction coefficient depends on the shape of the flow and the opening. For the flow directly through a sharp-edged opening, the contraction coefficient will be close to 0.6. For an opening with smooth rounded edges the coefficient will be close to 1. A typical value for the discharge coefficient for an envelope opening will be C_d = 0.65- 0.7.

1.4 Pressure loss in components and air flow paths

Relations between air flow and pressure loss through different ventilation components and air flow paths are necessary for determination of the ventilation capacity of a system. In natural and hybrid ventilation systems under design conditions the air flow will be turbulent or in the transition phase between laminar and turbulent. For conditions with lower air flow rates, laminar flow can occur and the relationship between pressure loss and volume flow rate becomes linear. Therefore, different models for estimation of the pressure loss through a component are often needed. Because of low velocities and often large temperature differences in the system stratified flow can occur in air channels and components. Under such conditions the relation between air flow and pressure loss can only be based on measurements. In the following the most

commonly used models are described.

1.4.1 Windows and other large openings

The air flow rate through windows and other large openings can be described by the following semi-empirical model, see section 1.3.:

$$q_v = C_d A \sqrt{\frac{2\Delta p}{\rho}} \qquad \text{Eq. 1.4.1}$$

where q_v is the air flow rate [m^3/s]
A is the geometrical opening area [m^2]
C_d is the discharge coefficient [-]
Δp is the pressure difference across the opening [Pa]
ρ is the air density of the air passing the opening [kg/m^3]

The value of the C_d depends on the contraction of the flow through the opening and the friction loss. For windows and other large openings friction will be negligible and the discharge coefficient typically falls in the range of 0,6 -0,7. for sharp-edged openings and approaching a value of 1,0 for rounded openings.

By rewriting Eq. 1.4.1 the pressure loss can be expressed as:

$$\Delta p = \frac{\rho}{2}\left(\frac{q_v}{C_d A}\right)^2 \qquad \text{Eq. 1.4.2}$$

1.4.2 Ventilation Components

Ventilation components are grilles, diffusers, heating coils, filters, etc. Two different models are used to describe the relation between air flow rate and pressure loss. An empirical power-law model can be used:

$$q_v = C\Delta p^n \qquad \text{Eq. 1.4.3}$$

where q_v is the air flow rate [m^3/s]
C is a characteristic flow coefficient [-]
Δp is the pressure difference across the component [Pa]
n is a dimensionless exponent [-]

Measured values of the flow coefficient for different components can be found in handbooks or from manufacturers. Measured exponents are in the range of 0.5 - 1.0, i.e. between turbulent and laminar air flow. Typically a value close to 0,6 is found.

A quadratic model can also be used:

$$\Delta p = \alpha q_v + \beta q_v^2 \qquad \text{Eq. 1.4.4}$$

where α,β are characteristic parameters for the component

Values for the parameters α and β for different components can be found in handbooks, from manufacturers or be estimated based on measurement data. The model combines a

linear relation suited for modelling of laminar air flows with a quadratic model suitable for modelling of turbulent air flows. Therefore, the model is often very useful for natural and hybrid ventilation applications, where air flow through components and air paths have characteristics of both flow types.

1.4.3 Air ducts and channels in buildings

The pressure loss in air ducts and channels in buildings can as a starting point be modelled by the standard expression for pressure loss in ducts:

$$\Delta p = f \frac{L}{D}\left(\frac{\rho q_v^2}{2A^2}\right) \qquad \text{Eq. 1.4.5}$$

where Δp is the pressure loss [Pa]
f is the friction factor [-]
L is the length of the duct/channel [m]
D is the hydraulic diameter [m]
q_v is the air flow rate [m^3/s]
A is the cross-sectional area [m^2]
ρ is the air density [kg/m^3]

The friction factor depends on the air flow conditions and can approximately be determined by:

Laminar air flow: $f = 16/\mathrm{Re}$ $\quad \mathrm{Re} < 2100$

Turbulent air flow: $f = 0.0791/\mathrm{Re}^{1/4}$ $\quad \mathrm{Re} > 2100$

Typical values for the friction factor in natural and hybrid systems are 0,01-0,05. The pressure loss should be designed to be negligible compared to other pressure losses in the system. It is important to take into consideration that stratified flow often exist in horizontal air ducts and channels because of low air velocities and temperature differences between the air and the duct surfaces. This will have an impact on both the pressure loss in the duct, but also on the pressure loss in connected components, as the velocity distribution of air flow through the components will not be even.

1.4.4 Fans

In hybrid systems the fan will in shorter or longer periods be off and provide a resistance to the flow corresponding to a negative pressure increase, $\Delta p_m^{\min}$. The relation between the air flow and the pressure difference can be modelled by the following equation, see /Feustel and Dieris/:

$$q_m^{\min} = a_1(-\Delta p_m^{\min})^{a_2} \qquad \text{(Eq. 1.4.6)}$$

where $q_m^{\min}$ is the air flow passing the stopped fan [m^3/s]
$\Delta p_m^{\min}$ is the pressure difference over the stopped fan [Pa]
a_1,a_2 are empirically determined coefficients

Equation (Eq. 1.4.6) can be rewritten as:

$$\Delta p_m^{\min} = -\left(\frac{q_m^{\min}}{a_1}\right)^{1/a_2} \qquad \text{(Eq. 1.4.7)}$$

Example 4

For an axial fan the following pressure-flow data applies, when it is stopped:

$q_m^{\min}$ $[m^3/s]$	*0.106*	*0.183*	*0.300*
$\Delta p_m^{\min}$ $[Pa]$	*-3*	*-5*	*-10*

By taking the logarithm of equation Eq. (1.4.6) it becomes:

$$\log(q_m^{\min}) = \log(a_1) + a_2 \log(-\Delta p_m^{\min})$$

The values of the coefficients a_1 and a_2 are obtained by linear regression using the above equation and the data in the table above. The following values are obtained: a_1 = 0.0431 and a_2 = 0.855. Eq. 1.4.7 then gives:

$$\Delta p_m^{\min} = -\left(\frac{q_m^{\min}}{0.0431}\right)^{1/0.855}$$

Figure 6 shows the modelled fan performance for different rotational speeds (including the pressure loss for 0 rpm) together with pressure flow data given in the tables. It can be seen from the figure that when a operating fan giving a resistance to the flow is stopped, the pressure loss will increase and the air flow rate decrease. This must be taken into consideration in the control strategy of the fan.

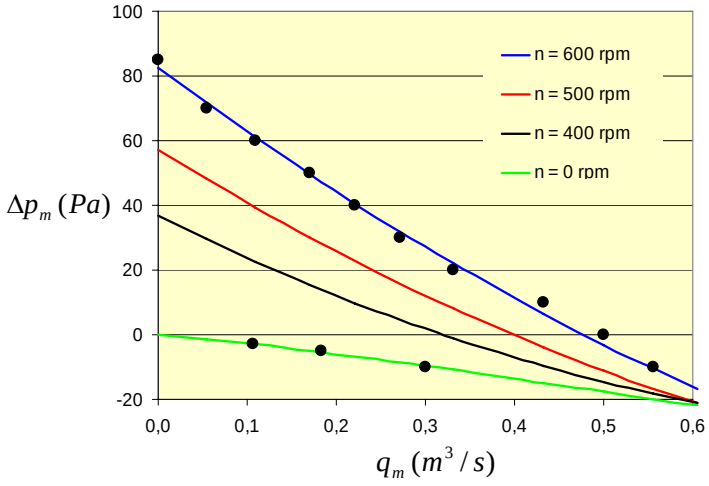

Figure 6. Modelled fan performance for different rotational speeds as well as pressure loss for a stopped fan compared with given pressure flow data.

1.4.5 Infiltration in cracks and leakages

An approximate value of the infiltration and exfiltration in buildings can be estimated by introducing the concept of effective leakagearea, A_l, which models the performance of several small leakage openings in the building construction. The model can be applied for evaluation of the sensitivity of the performance of the ventilation system with regard to infiltration. The air flow rate caused by infiltration can be calculated by:

$$q_v = A_l \sqrt{\frac{2\Delta p}{\rho}} \qquad \text{Eq. 1.4.8}$$

Estimation of the air flow by infiltration requires knowledge of the effective leakage area of the room and/or building. For existing buildings the effective leakage area can be found by measurements. For new designs the leakage area must be estimated. Tight buildings will typically have an infiltration air exchange rate of $n < 2\ h^{-1}$ at a pressure difference of 50 Pa (corresponding to the current requirements in the Danish Building Regulations), while it for less tight buildings can be $n > 10\ h^{-1}$. For very tight buildings following the voluntary energy standard "Passivhaus" the infiltration air exchange rate should be $n < 0{,}6\ h^{-1}$ at a pressure difference of 50 Pa.

Example 5

A school building is build as a tight construction with an infiltration air exchange rate of $n = 2\ h^{-1}$ at a pressure difference of 50 Pa. The effective leakage area of a classroom (Area 67,5 m^2, roomheight 2,7m) can be calculated by Eq. 1.4.8.

$$A_l = \frac{q_v}{\sqrt{\frac{2\Delta p}{\rho}}} = \frac{\frac{2h^{-1} \cdot (67{,}5m^2 \cdot 2{,}7m)}{3600s/h}}{\sqrt{\frac{2 \cdot 50\,pa}{1{,}2kg/m^3}}} = 0{,}011m^2$$

In order to calculate the infiltration rate in actual conditions is it necessary to determine the distribution of the effective leakage area on the room surfaces. This depends very much on the type of construction used. Typically the main leakage area is distributed around windows and doors as well as along edges between wall and roof construction and walls and floor constructions.

1.5 Prediction methods

According to the type of information needed, various prediction methods may be used. Methods range from very simple empirical algorithms to calculate the global air flow rate to sophisticated computerized fluid-dynamic techniques solving the Navier-Stokes equations. In general, based on the level of complexity, three different approaches can be distinguished for the description of the air flow in the case of natural ventilation of buildings.

- Analytical and empirical methods
- Network methods
- CFD methods

The first mentioned air flow prediction method is presented in the following chapters. It is important to note that use of deterministic methods to predict natural ventilation air

flow rates in buildings is based on assumptions that often fail to describe the actual conditions with sufficient accuracy. This affects the accuracy of the results obtained, as compared to measured values.

2 MODELLING OF NATURAL VENTILATION – SIMPLIFIED EMPIRICAL MODELS

Simplified empirical models offer general correlations to calculate the air flow rate in a zone. These expressions combine the air flow with the temperature difference, wind velocity and possibly a fluctuating term in order to give a bulk evaluation of the air flow rate in a building. These models are useful because they offer a fast first estimation of the air flow rate, but should always be used within the limits of their applicability. The following models have been deduced either from theory or from specific experimental data and cannot be considered of general validity.

2.1 Single-sided ventilation

Single-sided natural ventilation occurs in buildings or building zones with only one opening. This opening can be vertical or horizontal and ventilation can be driven by either thermal buoyancy or wind or a combination.

2.1.1 Ventilation through vertical opening due to thermal buoyancy.

For large openings with bidirectional flow the orifice model developed in section 1.3 is extended to cases where the opening height is not small in relation to the wall height and where the base pressure difference P_{u0}-P_{i0} is not determined by the conditions at one of the surfaces, but by the flow rate through the opening. This is the approach which has been most used in building physics. The main assumptions made when the orifice approach is applied to large openings are:

- Close to and within the aperture there is no mixing or heat transfer between the contra-flowing air streams.
- At the height of the neutral plane the pressures in both zones are equal.
- Streamlines are parallel and horizontal at the large opening. Vertical velocity component are small compared to the horizontal component.
- The viscous forces are small in comparison with those due to buoyancy (the Grashof number, Gr, is large).
- The pressure in the flow as it enters the receiving zone is equal to the hydrostatic pressure in that zone.

For a bidirectional flow, the same reasoning that lead to Eq. 1.1.2 and 1.3.2, applied along a streamline from a point in the room to a point in the opening gives the velocity in the parallel stream from the room to the outside as:

$$\Delta p = P_{i0} - P_{u0} + (\rho_u - \rho_i) g z = \rho_i \frac{u_i(z)^2}{2} \qquad \text{(Eq. 2.1.1)}$$

where $u_i(z)$ is the velocity in the indoor air leaving the room [m/s]

The position of the neutral height above the floor, H_n, is given by putting u(z) = 0, which gives the pressure difference between the zones at the reference level (floor) as:

$$P_{u0} - P_{i0} = (\rho_u - \rho_i) g H_n \qquad \text{(Eq. 2.1.2)}$$

The pressure differential inserted into the expressions for the velocities gives the velocity distribution in the two air streams:

$$\Delta p = (\rho_u - \rho_i) g (z - H_n) = \rho_i \frac{u_i(z)^2}{2} \qquad \text{(Eq. 2.1.3)}$$

$$u_i(z) = C_v \sqrt{\frac{2g}{\rho_i}(\rho_u - \rho_i)(z - H_n)} \qquad (z \geq H_n) \qquad \text{(Eq. 2.1.4)}$$

$$u_u(z) = C_v \sqrt{\frac{2g}{\rho_u}(\rho_u - \rho_i)(H_n - z)} \qquad (z \leq H_n) \qquad \text{(Eq. 2.1.5)}$$

where $u_u(z)$ is the velocity in the outdoor air flowing into the room [m/s]

$u_i(z)$ is the velocity in the indoor air flowing out of the room [m/s]

Due to contraction of the flow in the opening the maximum velocity in the opening can be calculated from:

$$u_{\max} = \sqrt{\frac{2g}{\rho_i}(\rho_u - \rho_i)(H_c - H_n)} = \sqrt{\frac{2g\Delta T}{\bar{T}}(H_c - H_n)} \qquad \text{(Eq. 2.1.6)}$$

It follows that the theoretical velocity profiles have a parabolic shape as shown in Figure 7.

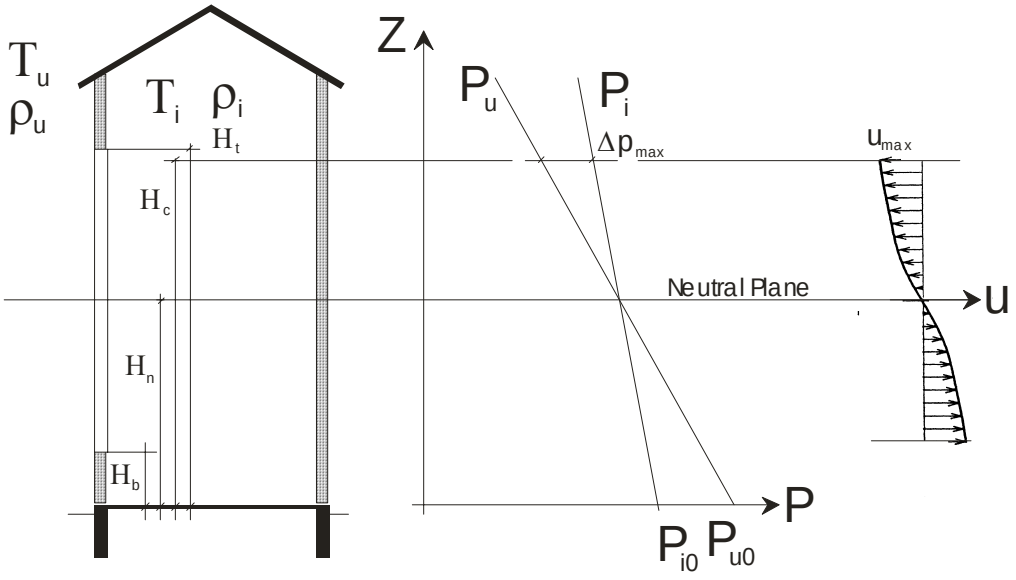

Figure 7. Pressure distribution and velocity profile for a single-sided opening.

The respective flows per unit width into and out of the room are, neglecting any contraction of the streamlines:

$$q_i = \int_{H_n}^{H_t} u_i(z)dz = \sqrt{\frac{2g}{\rho_i}(\rho_u - \rho_i)}\,\frac{2}{3}\left(H_t - H_n\right)^{3/2} \qquad \text{(Eq. 2.1.7)}$$

$$q_u = \int_{H_b}^{H_n} u_u(z)dz = \sqrt{\frac{2g}{\rho_u}(\rho_u - \rho_i)}\,\frac{2}{3}\left(H_n - H_b\right)^{3/2} \qquad \text{(Eq. 2.1.8)}$$

where q_i is the volume flow rate of indoor air leaving the room [m^3/s]
q_u is the volume flow rate of outdoor air flowing into the room [m^3/s]
H_t is the height of the top of the opening above the floor [m]
H_b is the height of the bottom of the opening above the floor [m]

Assuming mass conservation ($\rho_i q_i = \rho_u q_u$) one can solve for the neutral height in terms of the densities:

$$\frac{H_n - H_b}{H_t - H_n} = \left(\frac{\rho_i}{\rho_u}\right)^{1/3} \qquad \text{(Eq. 2.1.9)}$$

Because $\rho_t < \rho_u$ the neutral height will not be in the middle of the opening and the warmer air layer is thicker than the cool air layer. However, at the temperature differences normally encountered the difference will be less than 2%. If the neutral height is located in the middle of the opening and densities are interchanged with temperature according to (Eq 1.1.3) the total flow rate becomes:

$$q = \frac{1}{3}A\sqrt{\frac{g(T_i - T_u)(H_t - H_b)}{T_i}} \qquad \text{(Eq. 2.1.10)}$$

where q is the total air flow rate through the opening [m^3/s]
A is the opening area [m^2]

Since no account is taken in the above of streamline contraction, interfacial mixing, flow separation or viscous forces, it is necessary to replace the opening area, A, with the effective area, $A_{eff} = C_d A$, where C_d denotes the discharge coefficient.

Several authors have reported experimental values of the coefficient C_d in the literature for window and door openings, see Table 2. Most information is on doorways, and it is seen that there is a large variation from 0.4 to 0.8. It is not well understood was caused the differences. The algorithms developed assume that the flow is one-dimensional and that the interconnected room are at constant temperature. However, differences in experimental conditions might cause differences in the three-dimensional nature of the flow, in interfacial mixing at low temperature differences and in the presence of vertical temperature gradients, which might be some of the reasons for the discrepancies in the values of the discharge coefficient.

Table 2. Reported experimental values of the coefficient C_d in the literature.

	C_{dt}	Reference	Type of test
Window	0.61	Standard discharge coefficient for sharp-edged opening	-
	0.49-0.58	Mahajan and Hill (1986)	Two full-size adjoining rooms. A= 0,6m^2, ΔT=12 K. Measured velocity profile
Door	0.80	Shaw and Whyte (1974)	Two full-size adjoining rooms. A= 0.2-2.8m^2, ΔT=1-10 K. Measured velocity profile
	0.40 + 0.0045 ΔT	Kiel and Wilson (1989)	Outdoor testhouse, A=1.87m^2, ΔT=2-40 K. Tracer gas messurements
	0.6-0.75	Maas, Roulet and Hertig (1989)	Two full-size adjoining rooms. A=1.4m^2, ΔT=1.5+1.5z K. Measured velocity profile
	0.33-0.48	Mahajan and Hill (1986)	Two full-size adjoining rooms. A=1.37m^2, ΔT=12 K. Measured velocity profile
	0.62	Dalziel and Lane-Serff (1991)	Water model

Example 6

A room with the internal temperature of t_i = 22 ^{o}C has a single opening with the height of 1.5 m and the width of 1.2 m. The opening is located 0.6 m above the floor level. The external temperature is t_u = 10 ^{o}C.

The velocity profile in the opening can be calculated by Eq. (2.1.4):

$$u_i(z) = \sqrt{\frac{2g}{T_u}(T_i - T_u)(z - H_n)} \qquad (z \geq H_n)$$

With the neutral plane level in the middle of the opening the velocity profile becomes:

$$u_i(z) = \sqrt{\frac{2 \cdot 9.82}{(273+10}(22-10)(z-(0.6+1.5/2)} = \sqrt{0.83(z-1.35)}$$

The velocity profile is shown in Figure 8.

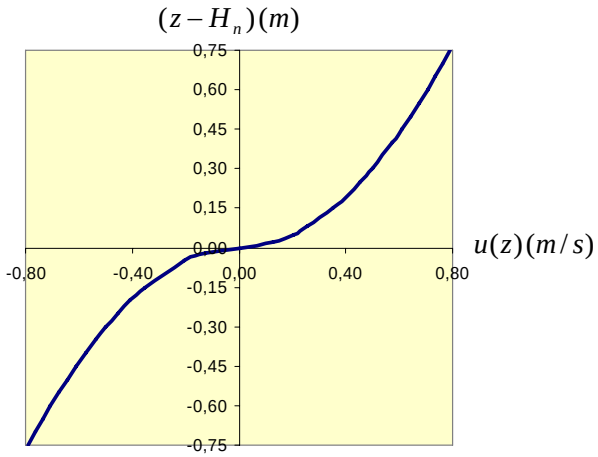

Figure 8. Predicted velocity profile for a single-sided opening.

The volume flow rate through the opening can be calculated from Eq. (2.1.10):

$$q = \frac{1}{3} A \sqrt{\frac{g(T_i - T_u)(H_t - H_b)}{\overline{T}}}$$

$$q = \frac{1}{3} \cdot (1.5 \cdot 1.2) \sqrt{\frac{9.82(22-10)(2.1-0.6)}{273 + \left(\frac{22+10}{2}\right)}} = 0.29 m^3/s$$

Figure 9 shows the volume flow rate through the opening per unit area as a function of opening height and temperature difference. Opening aspect area is an important parameter as high and narrow openings has a much higher capacity than low and wide openings. However, low openings can be easier to control as they give a more constant air flow rate for different temperature differences.

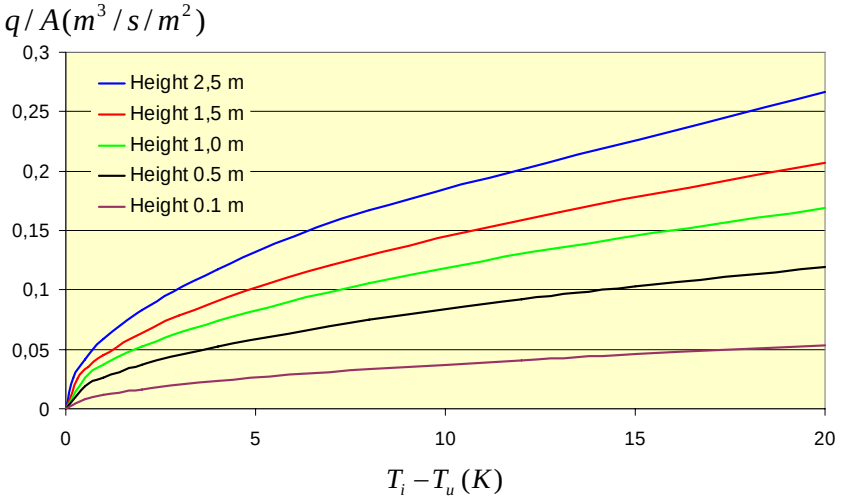

Figure 9. Volume flow rate per unit area as a function of opening height and temperature difference for a single-sided opening.

2.1.2 Ventilation through vertical openings due to wind.

This section deals with the case of a single opening in an otherwise sealed envelope exposed to a turbulent wind, which corresponds to an open window in a room where all other openings are relatively small. The steady flow model cannot deal with such case, because the mean pressure difference across the opening is equal to zero, yet an effective ventilation rate occurs as a result of turbulence and/or local pressure differences. The wind ventilation can be subdivided into three components – steady-state ventilation, ventilation by turbulent eddy penetration and ventilation by pulsation flow, Malinnowski (1971).

A major difficulty is that the interaction between the turbulence and the geometry of the opening can be very complicated. When Δp is small in relation to the external pressure fluctuation it can be expected that turbulence will generate a significant time-averaged effective flow rate. Both the external velocity field and the pressure field near the opening can be important. The relative importance of these two effects depends partly on the overall size of the opening in relation to the length scales of the external turbulence. This can be seen by considering the three types of openings shown in Figure 10, namely a fully open window, a closed window and a small air vent. Considering the air vent first, the external pressure at any time will be uniform across the opening when the size of the opening is small in relation to the length scales of the turbulent pressure fluctuations. For the closed window and the open window, the external pressure at a given instant is less likely to be uniform over the open area. The correlations between pressures at different positions around the opening are therefore likely to have an effect on the ventilation flows. For the open window there is a further complication in that the size of the opening is large enough for the external velocity field to be modified, i.e. turbulent motion in a direction normal to the wall can transport air through the opening even when the pressure difference is negligible. For the two other openings the velocities close to the wall remain small as the air flows past the opening.

Large eddies in the external flow can penetrate the large opening, leading to bidirectional flow. Only small eddies can penetrate small openings, and if their depth is of similar size to their width, the penetration might not lead to significant ventilation. Bidirectional flow can occur with the closed window as a result of non-uniform external pressure, but it is much less likely with the small opening.

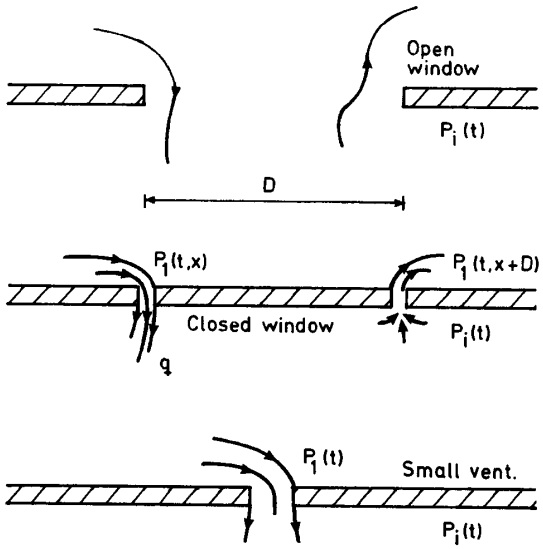

Figure 10. Possible flows induced by external turbulence for three types of opening. (Etheridge and Sandberg, 1996).

For a given building the air flow rate due to the wind through a single opening in the surface of the building will be a function of the following parameters:

- Reference wind speed, v_{ref}, wind direction, θ and turbulence.
- Opening area, *A*, opening geometry and position of the opening on the building façade.
- The shape and surroundings of the building

For simplification one can make the assumption that the flow is independent of viscosity (which is not unreasonable for a large opening) and that the ventilated space in the single-sided ventilation case is isolated from the remainder of the building and the air flow rate therefore only depends on local conditions at the opening, which include:

- The local air speed, v_L, assumed to be parallel to the surface, which is reasonable as the dimensions of a typical window will be small compared to the dimensions of the building itself.
- The local direction, β, of the air flow in a plane parallel to the surface and the turbulent length scale
- The surface pressure characteristics.

This will allow the following equations to be written, Warren (1977) and Warren and Parkins (1985):

$$\frac{v_L}{v_{ref}} = f\left\{(building\quad characteristics),(opening\quad location),(wind\quad direction)\right\} \quad \text{(Eq. 2.1.11)}$$

$$\frac{q}{Av_L} = f\left\{(\mathrm{Re}),\beta,(turbulent\quad lenght\quad scale),(geometry\quad of\quad opening)\right\} = F_L \quad \text{(Eq. 2.1.12)}$$

The dimensionless air flow rate is called the Flow number, F, with a subscript corresponding to the reference speed used.

A few authors have reported experimental values of the flow number in the literature for window openings, see Table 3.

Table 3. Reported experimental values of the flow number in the literature.

Type	Value	Reference	Type of test
F_L	0.130 (A=0.0225m^2) 0.096 (A=0.0529m^2) 0.090 (A=0.0900m^2)	Brown and Solvason (1962)	Laboratory, fan created flow
F_L	0.025 (Tu = 0.8%) 0.035 (Tu = 9.0%)	Warren (1977)	Windtunnel (v_L=1.1-5.2m/s) A=0.013 – 0.065 m^2 Tracer gas measurements
F_L	0.105	Warren (1977)	Outdoor testhouse, A=0.15m^2. v_L/v_{ref} = 0.2 (θ=0^o) – 0.6 Tracer gas measurements
F_{ref}	0.021 – 0.063		
F_{ref}	0.025	Warren and Parkins (1985)	Outdoor testhouse, A=0.15m^2. Tracer gas measurements
F_{ref}	0.05 – 0.15	Maas (1992)	Outdoor testhouse, A=0.01 – 0.02m^2. V_{ref} = 5.1 – 10.2 m/s Tracer gas measurements
F_{ref}	0.025 – 0.04	Crommelin and Vrins (1988)	Windtunnel, A = 0.0019 – 0.0225 m^2. V_{ref} = 2 – 9 m/s Tracer gas measurements

The results show a large variation, which can be attributed to variations of a number of parameters like opening shape, wind direction, turbulence level, turbulent length scale, etc., in the flow, that probably has a large effect. Narasaki et al (1989) investigated the influence of these parameters in a series of windtunnel experiments and found out:

- that the air flow rate was proportional to the local wind speed for small aspect ratios, but not when the opening aspect ratio was larger than 8 – 16
- that the air flow rate depended on wind direction, but the dependence was different for different opening aspect ratios and turbulence levels
- that the air flow rate was proportional to the turbulence level

2.1.3 Ventilation through vertical opening due to thermal buoyancy and wind.

The effect of buoyancy and wind on the flow through various types of windows has been investigated by de Gids and Phaff (1982). They developed a general expression for

the ventilation air flow rate through an open window as a function of temperature difference, wind velocity and fluctuating terms. An effective velocity, v_{eff}, is defined and refers to the flow through half a window opening. In a general form the effective velocity is defined as:

$$v_{eff} = \frac{q}{A/2} = \sqrt{\frac{2}{\rho}(\Delta p_{wind} + \Delta p_{stack} + \Delta p_{turb})} \qquad \text{(Eq. 2.1.13)}$$

leading to the form:

$$v_{eff} = \frac{q}{A/2} = \sqrt{C_1 v_{ref}^2 + C_2(H_t - H_b)(T_i - T_u) + C_3} \qquad \text{(Eq. 2.1.14)}$$

where C_1 is a dimensionless coefficient depending on the wind [-]
C_2 is a constant depending on thermal buoyancy [-]
C_3 is a constant depending on wind turbulence [-]

The term C_3 is equivalent to an effective turbulence pressure that provides ventilation in the absence of stack effect or steady wind.

Using the effective velocity as given by Eq. 2.1.13, the flow rate through the window is given by:

$$q = \frac{A}{2} v_{eff} \qquad \text{(Eq. 2.1.15)}$$

where A is the effective window opening area [m^2]

From a total of 33 air change measurements on site, de Gids and Phaff (1982) obtained the following values for the constants: C_1 = 0.001, C_2 = 0.0035 and C_3 = 0.01. The final equation for flow rate through an open window due to both buoyancy and wind becomes:

$$q = \frac{A}{2}\sqrt{0.001 v_{ref}^2 + 0.0035(H_t - H_b)(T_i - T_u) + 0.01} \qquad \text{(Eq. 2.1.16)}$$

In the 33 measurements the influence of various window types (vertically pivoted, casement windows, horizontally pivoted vent lights and a sash window) and of window height/width ratios on air change rates was investigated, but no clear distinctions could be made for these variables.

Other experimental investigations, Maas (1992), have found by experiments that the ventilation produced by combining wind and thermal buoyancy is not systematically larger than the thermal buoyancy separately, which is in disagreement with Eq. 2.1.14.

From a series of wind tunnel experiments Larsen et al. (2003) concluded that the volume flow through the opening also changes with the wind direction. Figure 11 shows measured air flow rates through a single sided vertical opening due to thermal buoyancy and wind. The measurements were performed in a large open wind tunnel on a full-scale building which was rotated to measure the air change rate at different wind directions. The opening area was 1.2 m^2 (height 1.4 m, width 0.86m) and the opening was placed in a test room with the dimensions length 5.56 m, width 5.56 m and height 3.0m.

Figure 11 shows that the volume flow rates are dependent on the wind direction. This dependence is smaller when the opening is located on the leeward side of the building (angle 180°). It is also shown that the models developed by Warren and Parkins (1985) and de Gids and Phaff (1982), gives a reasonable average level of the flow rate for the range of application and that the value is most accurate for openings located on the leeward side of the building. To improve the models it will be necessary to develop new expressions, where the variations for different incidence angles are included.

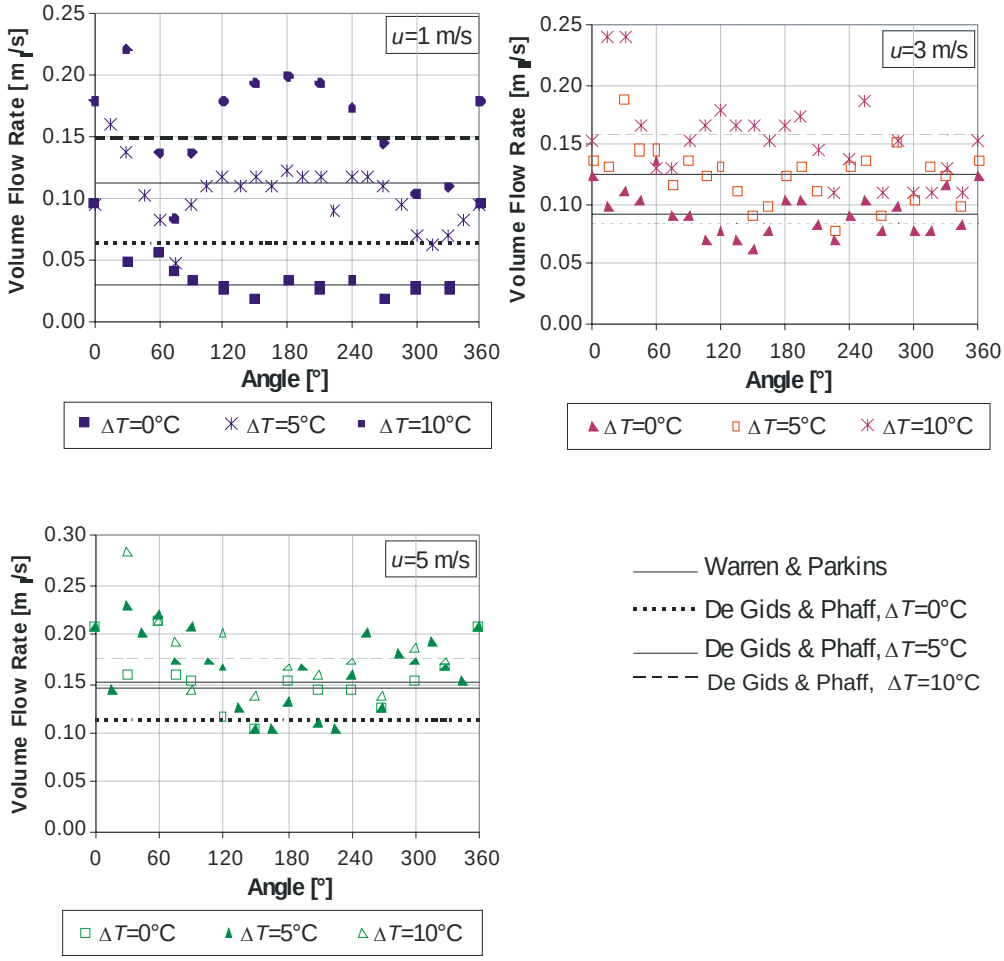

Figure 11. Measured and calculated air flow rates through a single sided vertical opening due to thermal buoyancy and wind.(Larsen et al. 2003).

2.1.4 Ventilation through horizontal opening due to thermal buoyancy.

In a situation with a horizontal opening between a warm room below and a cool environment the density difference makes for a buoyancy-driven downflow of heavier air into the room and if the room is sealed mass conservation dictates an upflow of lighter air. In the case of a single opening, this gives rise to an oscillatory, see Figure 12, or countercurrent exchange flow across the opening depending on the relation between opening height and opening diameter, *h/D*.

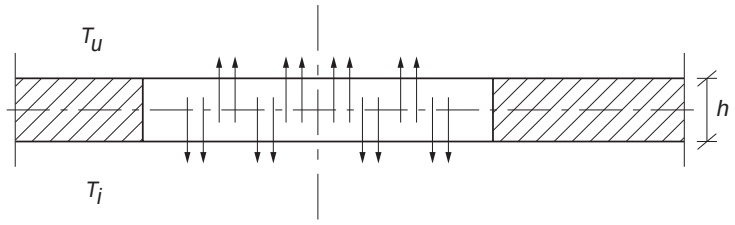

Figure 12. Countercurrent exchange flow across a horizontal opening.

At very small opening heights the pressure level on both sides of the opening is essentially the same and an oscillatory exchange flow regime will be established. Based on experimental investigations Epstein (1988) found the following empirical relation for the air flow rate through the opening:

$$q = 0{,}055\sqrt{\frac{g(T_i - T_u)D^5}{T_i}} \quad \text{for } h/D < 0{,}15 \qquad \text{(Eq. 2.1.17)}$$

For larger values of *h/D* the flow regime change from an countercurrent orifice flow regime ($0{,}15 < h/D < 0{,}4$) to a turbulent diffusion flow regime for very large values ($3{,}25 < h/D$). In the turbulent diffusion flow regime the air exchange was much slower and the countercurrent flow within the tube appeared to comprise of packets of warm and cold air with a chaotic and random motion. For intermediate values ($0{,}4 < h/D^{½} < 3{,}25$) the flow will be a combination of an orifice flow and turbulent diffusion flow regime. Based on scale model data from Brown (1962), Mercer and Thompson (1975) and own data, Epstein (1988) developed the following relation for air flow rate through the opening:

$$q = 0{,}147\sqrt{\frac{g(T_i - T_u)D^5}{T_i}}\left(\frac{h}{D}\right)^{½} \quad \text{for } 0{,}15 < h/D < 0{,}4 \qquad \text{(Eq. 2.1.18)}$$

$$q = 0{,}093\sqrt{\frac{g(T_i - T_u)D^5}{T_i}}\frac{1}{\sqrt{1 + 0{,}084\left(\frac{h}{D} - 0{,}4\right)^3}} \quad \text{for } 0{,}4 < h/D < 3{,}25 \qquad \text{(Eq. 2.1.19)}$$

$$q = 0{,}32\sqrt{\frac{g(T_i - T_u)D^5}{T_i}}\left(\frac{h}{D}\right)^{3/2} \quad \text{for } 3{,}25 < h/D < 20 \qquad \text{(Eq. 2.1.20)}$$

For square openings with a side length S, D should be viewed as the diameter that a round opening would attain if it had the same area as the square opening described by the following relation:

$$D = \sqrt{\frac{4}{\pi}S^2} = 1.128 \cdot S \qquad \text{(Eq. 2.1.21)}$$

Epstein (1988) developed the following purely empirical correlation for the air flow rate over the entire range of h/D:

$$q = 0{,}055\sqrt{\frac{g(T_i - T_u)D^5}{T_i}}\frac{\left(1+400\left(\frac{h}{D}\right)^3\right)^{1/6}}{\left(1+0{,}00527\left(1+400\left(\frac{h}{D}\right)^3\right)^{1/2}\left(\left(\frac{h}{D}\right)^6+117\left(\frac{h}{D}\right)^2\right)^{3/4}\right)^{1/3}} \quad \text{(Eq. 2.1.22)}$$

The dimensionless air flow rate through a single horizontal opening as a function of *h/D* is shown in Figure 13. Eq. (2.1.22) shows a reasonable correspondence with Eq. (2.1.17) – Eq. (2.1.20).

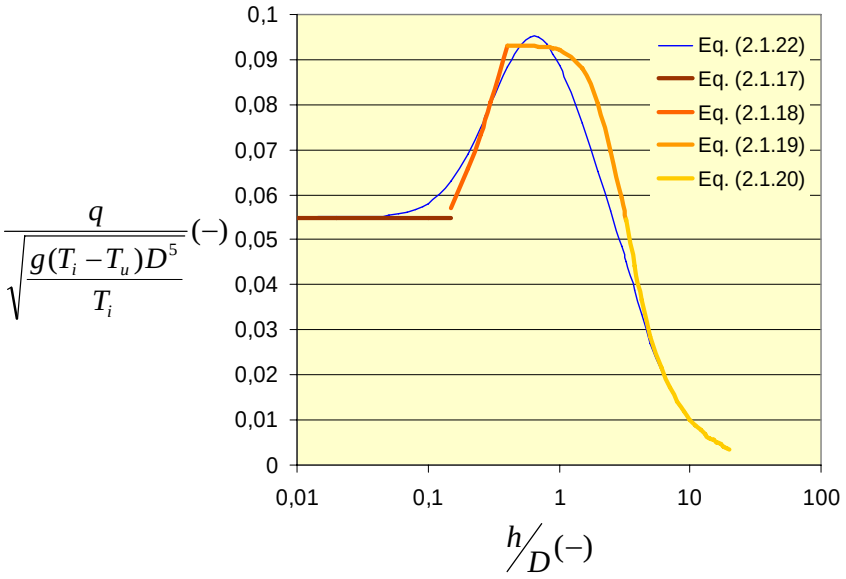

Figure 13. Dimensionless air flow rate through a single horizontal opening as a function of h/D of the opening, Eq (2.1.22).

Eq. 2.1.17 was confirmed by scale model measurements by Conover et al., 1995 as well as Sandberg and Blomqvist (2002), which found values of the coefficient from 0,035 to 0,047. However, in a number of full scale experiments with air by Blay et al. (1998) and Kohal et al, (1994) measured air flow rates for values of $h/A^{1/2}$ between 0,4 and 1,4 that were 2-3 times higher, than predicted by Eq. 2.1.19.

Li et al. (2004, 2005a) investigated buoyancy driven natural ventilation through single-sided horizontal openings in a full-scale laboratory test rig. The measurements were made for opening ratios *h/D* ranging from 0.115 to 4.455. The dimensionless air flow rates measured are compared with calculated air flow rates by Eq. 2.1.17 – 2.1.20 in Figure 14. The results show that it is not possible to distinguish between four different flow regimes. A constant dimensionless air flow rate was not found for the values of *h/D* below 0,15 and the values found were less than 0.55. The maximum dimensionless air flow rate was not found for *h/D* = 0,4, but for *h/D* = 0,6. The maximum dimensionless air flow rate was also found to be approximately 20% higher than predicted by Eq. 2.1.19. Based on the results two new relations were developed:

$$q = 0.141\sqrt{\frac{g(T_i - T_u)L^5}{T_i}}\left(\frac{h}{D}\right)^{0,502} \qquad 0.115 < \frac{L}{D} < 0.6 \qquad \text{(Eq. 2.1.23)}$$

$$q = 0.084\sqrt{\frac{g(T_i - T_u)L^5}{T_i}}\left(\frac{h}{D}\right)^{-0,541} \qquad 0.6 < \frac{L}{D} < 4.455 \qquad \text{(Eq. 2.1.24)}$$

The two new models are also shown in Figure 14.

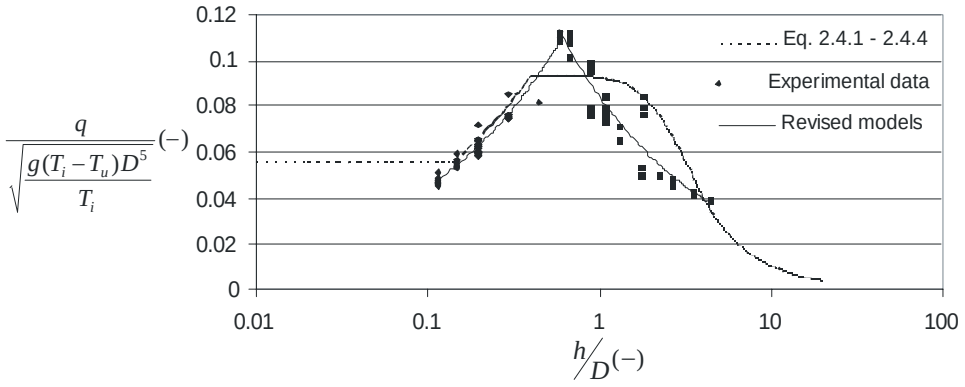

Figure 14. Measured dimensionless air flow rate as a function of h/D compared with Eq. 2.4.1 – 2.4.4 and a new revised model.

2.2 Single Zone Ventilation by thermal buoyancy

Single zone ventilation can be calculated by the mass balance method. The calculation of the air flow rates through openings in the zone is based on the equation of mass-balance for the zone with the internal pressure as the unknown. When the internal pressure is known the air flow rates through the individual openings can be calculated as well as the air flow rate of the whole system

2.2.1 Ventilation through two separate openings

The simplest case involves only two small rectangular openings placed above each other as shown on Figure 15. The inside temperature is constant. Balance equations for energy, mass and momentum as well as equations for the relationship between pressure differences and air velocities and between density and temperature differences can be used to estimate the pressure differences between outside and inside and air velocities through the openings.

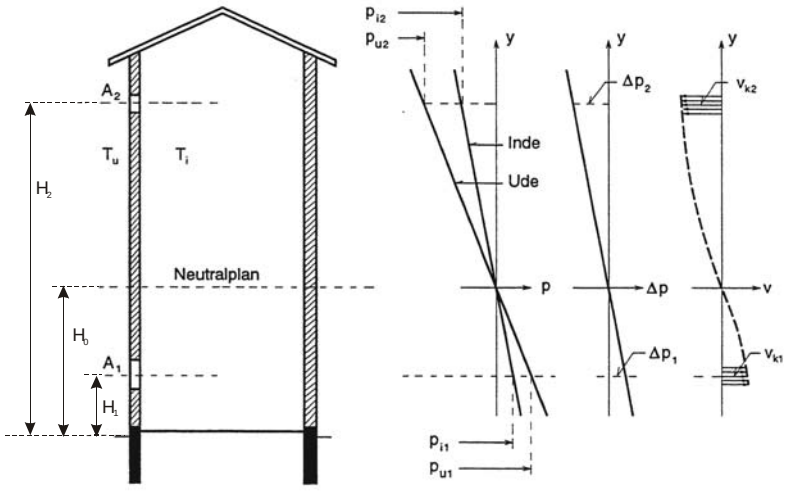

Figure 15. Thermal buoyancy in a room with two openings as well as pressure and velocity conditions. (Andersen 1998).

Figure 15 shows, because of a under pressure compared to the outside at the lower opening and an over pressure at the higher opening, that air flows from the outside to the inside in the lower opening and from the inside to the outside in the higher opening. Somewhere between the openings there will be a horizontal plane called the neutral plane where inside and outside pressures are equal.

Eq. 1.1.2 gives the expression for the pressure difference *Δp* across an opening at the height H:

$$\Delta p = P_{u0} - P_{i0} - gH(\rho_u - \rho_i) \qquad \text{(Eq. 2.2.1)}$$

When temperature differences are not large (<30K) the temperature and density differences are approximately related by:

$$\frac{\rho_u - \rho_i}{\rho_u} \cong \frac{T_i - T_u}{T_i} \qquad \text{(Eq. 2.2.2)}$$

The position of the neutral height above the floor, H_n, is given by putting $\Delta p = 0$, which gives the pressure difference between the zones at the reference level (floor) as:

$$P_{u0} - P_{i0} = \rho_u g H_o \frac{T_i - T_u}{T_i} \qquad \text{(Eq. 2.2.3)}$$

The pressure difference for an opening of height H_1 becomes:

$$\Delta p_1 = P_{u0} - P_{i0} - \rho_u g H_1 \frac{T_i - T_u}{T_i} \qquad \text{(Eq. 2.2.4)}$$

$$\Delta p_1 = \rho_u g H_o \frac{T_i - T_u}{T_i} - \rho_u g H_1 \frac{T_i - T_u}{T_i} = \rho_u g \frac{T_i - T_u}{T_i}\left(H_o - H_1\right) \qquad \text{(Eq. 2.2.5)}$$

It is seen that for openings below the neutral plane the pressure difference is positive and for openings above the neutral plane the pressure difference is negative. The air flow rate through and opening can be calculated from Eq. 1.2.11:

$$q = C_d A v_{theo} = C_d A \sqrt{\frac{2|\Delta p|}{\rho}} \frac{\Delta p}{|\Delta p|} \qquad \text{(Eq. 2.2.6)}$$

The level of the neutral plane is determined by the mass balance, so the amount of inward air flow equals the amount of outward air flow. If the two openings have the same area the neutral plane will be located in the middle. If the area of the openings is not the same, the position can be determined from the mass balance where the position of the neutral plane is the only unknown:

$$\rho_u q_{v1} - \rho_i q_{v2} = 0 \qquad \text{(Eq. 2.2.7)}$$

$\Leftrightarrow$

$$\rho_u C_{d1} A_1 \left(\frac{2\Delta T g (H_o - H_1)}{T_i} \right)^{1/2} - \rho_i C_{d2} A_2 \left(\frac{2\Delta T g (H_2 - H_o)}{T_u} \right)^{1/2} = 0 \qquad \text{(Eq. 2.2.8)}$$

where

ρ_u, ρ_i	is the density of outdoor and indoor air (kg/m^3)
q_{v1}, q_{v2}	is the air flow rates through the inlet and outlet (m^3/s)
C_{d1}, C_{d2}	is the discharge coefficient of inlet and outlet openings
A_1,A_2	is the inlet and outlet area (m^2)
ΔT	is the temperature difference between the inside and outside, (T_i-T_u) (°C)
g	is the gravitational acceleration (m/s^2)
T_i, T_u	is the absolute indoor and outdoor temperature (K)
H_1, H_2	is height of the inlet and the outlet opening (m)
H_0	is height of the neutral plane (m)

The inlet and outlet openings will often be of the same type and then $C_{d1} \sim C_{d2}$. The equation can be reduced to:

$$A_1 (H_0 - H_1)^{1/2} - A_2 (H_2 - H_0)^{1/2} = 0 \qquad \text{(Eq. 2.2.9)}$$

$\Leftrightarrow$

$$H_0 = \frac{A_1^2 H_1 + A_2^2 H_2}{A_1^2 + A_2^2} \qquad \text{(Eq. 2.2.10)}$$

When the position of the neutral plane is known pressure differences, air velocities as well as ventilation capacity can be calculated by the above equations. The equations can also be used for a number of openings if they are positioned only in two heights. The inlet area will then be the total area of openings at low level and the outlet area the total area of openings at high level.

The discharge coefficients include both friction loss and contraction in the openings.

For window openings it will be between 0.6 – 0.75 with the lowest value for sharp-edged openings. The friction number will be between 0,05- 0,1.

For a single zone with two openings the calculation of the air flow rate can be simplified by introducing the effective opening area, A^*, (Andersen 2003):

$$q_v = C_d A^* \sqrt{\frac{2gh(T_i - T_o)}{T_o}} \qquad \text{(Eq. 2.2.11)}$$

$$A^* = \frac{A_T \cdot A_B}{\sqrt{A_T^2 + A_B^2}} \qquad \text{(Eq. 2.2.12)}$$

where q_v is the air flow rate [m^3/s],
A^* is the effective opening area [m^2],
A_T is the area of the top opening [m^2],
A_B is the area of the bottom opening [m^2],
g is the gravitational acceleration [m/s^2],
T_i is the inside temperature [K],
T_o is the outside temperature [K],
h is the vertical distance between the two openings [m]
C_d is the discharge coefficient of the openings

The above equations are valid if the air flow through the openings is unidirectional. If difference in opening area between the top and the bottom opening becomes large, two directional air flow will occur in one of the openings and the predicted air flow rate be too low.

Li et al. (2005b) has investigated this phenomenon in a full scale experiment. The measurement were performed for opening ratios between $0.11 < A_T/A_B < 25$. Smoke visualization showed that three flow modes could be identified: bidirectional flow through the bottom opening, one directional flow through the two openings and bidirectional flow through the top opening, depending on the different A_T/A_B values. Figure 16 shows the relation between measured and predicted air flow rate, q_m/q_v, as a function of opening ratio A_T/A_B, (a) in the range of $0.11 < A_T/A_B < 2$ and (b) in the range of $2 < A_T/A_B < 25$. It is seen that the above approach is valid for an opening area ratio between 0.3 – 11.

(a)

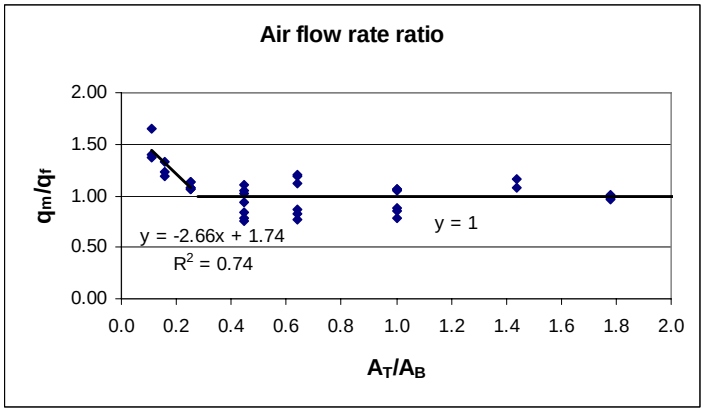

(b)

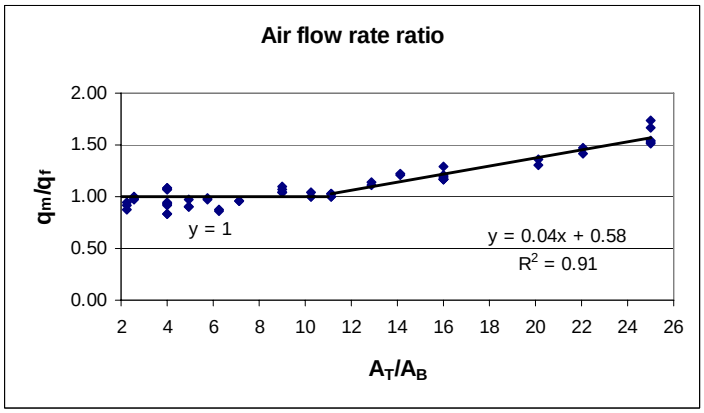

Figure 16. The relation between measured and predicted air flow rate, q_m/q_v, as a function of opening ratio A_T/A_B, (A) in the range of $0.11 < A_T/A_B < 2$ and (B) in the range of $2 < A_T/A_B < 25$.Li et al. (2005b).

According to the relationship between the air flow rate ratio q_m/q_f and the opening ratio A_T/A_B, new empirical models for calculation of the air flow rate can be obtained. By introducing an opening area ratio factor, C_A, which is a linear function of A_T/A_B, the new model can be expressed as:

$$q = C_A C_d A^* \sqrt{\frac{2gh(T_i - T_o)}{T_o}}$$

$$C_A = -2.66\frac{A_T}{A_B} + 1.74 \qquad 0.11 < \frac{A_T}{A_B} < 0.28$$

$$C_A = 1 \qquad 0.28 < \frac{A_T}{A_B} < 11 \qquad \text{(Eq. 2.2.13)}$$

$$C_A = 0.04\frac{A_T}{A_B} + 0.58 \qquad 11 < \frac{A_T}{A_B} < 25$$

2.2.2 Ventilation through several separate openings

Openings in more than two levels as it is shown in Figure 17 will not change the interior pressure distribution, but the location of the neutral plane must be known to be able to calculate the pressure difference across the openings and thereby the air velocities and air flow rates.

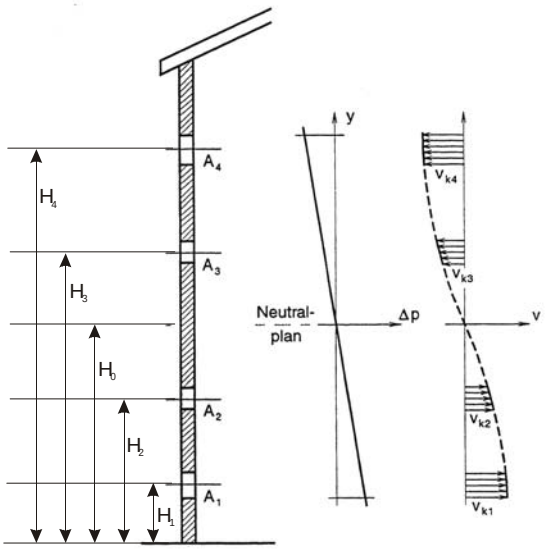

Figure 17. Pressure differences and air velocities by thermal buoyancy in a room with four openings. (Andersen 1998).

The location of the neutral plane is determined from the mass balance, as it was the case for two openings. If it is assumed as a first guess that the neutral plane is situated between opening 2 and 3 the mass balance for the four openings in Figure 17 will be:

$$\rho_u q_{v1} + \rho_u q_{v2} - \rho_i q_{v3} - \rho_i q_{v4} = 0 \qquad \text{(Eq. 2.2.14)}$$

$\Leftrightarrow$

$$\rho_u C_{d1} A_1 \left(\frac{2\Delta T g (H_0 - H_1)}{T_i} \right)^{1/2} + \rho_u C_{d2} A_2 \left(\frac{2\Delta T g (H_0 - H_2)}{T_i} \right)^{1/2} - \rho_i C_{d3} A_3 \left(\frac{2\Delta T g (H_3 - H_0)}{T_u} \right)^{1/2} -$$

$$\rho_i C_{d4} A_4 \left(\frac{2\Delta T g (H_4 - H_0)}{T_u} \right)^{1/2} = 0$$

where the location of the neutral plane is the only unknown. If it is assumed as for two openings that $C_{d1} \sim C_{d2} \sim C_{d3} \sim C_{d4}$ the equation can be reduced to:

$$A_1 (H_0 - H_1)^{1/2} + A_2 ((H_0 - H_2))^{1/2} - A_3 ((H_3 - H_0))^{1/2} - A_4 ((H_4 - H_0))^{1/2} = 0 \qquad \text{(Eq. 2.2.15)}$$

or in a general form:

$$\sum_{j=1}^{n} A_j \left| H_o - H_j \right|^{1/2} \frac{H_o - H_j}{\left| H_o - H_j \right|} = 0 \qquad \text{(Eq. 2.2.16)}$$

The equation can be solved by iteration. A good first guess on the position of the neutral plane is usually found by only taking the lowest and the highest opening into consideration as they contribute the most to the mass balance. If the neutral plane is located at one of the openings this opening is omitted in the next step of the iteration, as the contribution from this opening to the mass balance will be negligible. When the location of the neutral plane is determined the pressure difference across each opening because of thermal stack effect can be calculated as:

$$\Delta p_T = \Delta\rho g(H_0 - H) = \frac{\rho_o \Delta T}{T_i} g(H_0 - H) \qquad \text{(Eq. 2.2.17)}$$

where H is the height of the specific opening (m)

With a known pressure difference the air velocity and the ventilation air flow rate can be calculated. If it is assumed in the case of four openings in Figure 17 that the position of the neutral plane is between opening 2 and 3 the ventilation capacity can be calculated as:

$$q_v = C_{d1}A_1\left(\frac{2\Delta p_{T1}}{\rho_u}\right)^{1/2} + C_{d2}A_2\left(\frac{2\Delta p_{T2}}{\rho_u}\right)^{1/2} \text{ (m}^3\text{/s)} \qquad \text{(Eq. 2.2.18)}$$

$\Leftrightarrow$

$$q_v = C_{d1}A_1\left(\frac{2\Delta T g|H_1 - H_0|}{T_i}\right)^{1/2} + C_{d2}A_2\left(\frac{2\Delta T g|H_2 - H_0|}{T_i}\right)^{1/2} \text{ (m}^3\text{/s)} \qquad \text{(Eq. 2.2.19)}$$

2.3 Single Zone Ventilation by wind

The pressure difference across an opening can be calculated as:

$$\Delta p = P_w - P_i \quad \Leftrightarrow \quad \Delta p = \tfrac{1}{2} C_p \rho_u v_{ref}^2 - P_i \qquad \text{(Eq. 2.3.1)}$$

where P_i is the internal pressure in the building (Pa)

The internal pressure can be found from the mass balance.

$$\sum \rho_u C_{d1} A_1 v_{theo,1} = \sum \rho_i C_{d2} A_2 v_{theo,2} \qquad \text{(Eq. 2.3.2)}$$

where index 1 refers to inlet opening and index 2 refers to outlet openings. The theoretical velocity (when friction loss is not taken into consideration) through an opening can be calculated as:

$$v_{theo,i} = \sqrt{\frac{2\Delta p}{\rho}} \qquad \text{(Eq. 2.3.3)}$$

where ρ is the density of outside air for inlet openings and the density of inside air for outlet openings (kg/m^3)

Equation (2.3.2) can then be rewritten as:

$$\sum \rho_u C_{d1} A_1 \left(\frac{\left| C_{p1} \rho_u v_{ref}^2 - 2P_i \right|}{\rho_u} \right)^{1/2} = \sum \rho_i C_{d2} A_2 \left(\frac{\left| C_{p2} \rho_u v_{ref}^2 - 2P_i \right|}{\rho_i} \right)^{1/2} \quad \text{(Eq. 2.3.4)}$$

where P_i is the only unknown that can be found by an iterative solution method.

For the special situation with only two openings P_i can be calculated as:

$$P_i = \tfrac{1}{2} \rho_u v_{ref}^2 \frac{C_{p2} + \frac{\rho_u C_{d1}^2 A_1^2}{\rho_i C_{d2}^2 A_2^2} C_{p1}}{1 + \frac{\rho_u C_{d1}^2 A_1^2}{\rho_i C_{d2}^2 A_2^2}} \quad \text{Eq. 2.3.5)}$$

If it is assumed that $C_{d1} \sim C_{d2}$ and $\rho_u \sim \rho_i$ the equation can be reduced to:

$$P_i = \tfrac{1}{2} \rho_u v_{ref}^2 \frac{A_1^2 C_{p1} + A_2^2 C_{p2}}{A_1^2 + A_2^2} \quad \text{Eq. 2.3.6}$$

The mass balance can also be written in a general form as:

$$\sum_{j=1}^{n} C_{d,j} A_j \rho_j \left(\frac{\left| \Delta p_j \right|}{\tfrac{1}{2} \rho_j} \right)^{1/2} \frac{\Delta p_j}{\left| \Delta p_j \right|} = 0 \quad \text{(Eq. 2.3.7)}$$

where index j denotes each opening in the building and Δp_j is calculated from equation (2.3.1) for each opening. The last factor in the equation determines the type of opening as it will be 1 for inlet openings and –1 for outlet openings.

When the internal pressure is known the ventilation capacity can be calculated as the total air flow through all openings divided by 2:

$$q_v = \tfrac{1}{2} \sum_{j=1}^{n} C_{d,j} A_j \left(\frac{\left| \tfrac{1}{2} C_{p,j} \rho_u v_{ref}^2 - P_i \right|}{\tfrac{1}{2} \rho_j} \right)^{1/2} \text{(m}^3\text{/s)} \quad \text{(Eq. 2.3.8)}$$

The wind pressures in this calculation method are regarded as steady which naturally is a rough simplification. Natural wind is turbulent and wind pressures will be fluctuating. Investigations show that wind turbulence can cause of a considerable increase in ventilation capacity compared to the situation with steady wind velocity and –direction as in the calculations.

2.4 Single Zone Ventilation by a combination of thermal buoyancy and wind

In reality it will always be a combination of thermal buoyancy and wind forces that drive natural ventilation. The total pressure difference across an opening will then be the sum of pressure differences. To be able to calculate the individual contributions it is necessary to find the location of the neutral plane as well as the internal pressure in the

building.

The neutral plane can be found from the mass balance, Eq. (2.2.15), which is solved by iteration for H_0:

$$\sum_{j=1}^{n} A_j \left|H_o - H_j\right|^{½} \frac{H_o - H_j}{\left|H_o - H_j\right|} = 0 \qquad \text{(Eq. 2.4.1)}$$

where index j refers to either inlet openings or outlet openings.

The pressure difference by thermal buoyancy can be found from Eq. (2.2.17) and the pressure difference because of wind forces by Eq. (2.3.1). The total pressure difference across the opening will be the sum of the two components:

$$\Delta p = \Delta p_w + \Delta p_T = ½ C_p \rho_u v_{ref}^2 - P_i + \frac{\rho_u \Delta T}{T_i} g(H_0 - H) \qquad \text{(Eq. 2.4.2)}$$

The internal pressure at height, H_o, can be found from the mass balance, Eq. (2.3.5) by an iterative solution method:

$$\sum_{j=1}^{n} C_{d,j} A_j \rho_j \left(\frac{\left|\Delta p_j\right|}{½ \rho_j} \right)^{½} \frac{\Delta p_j}{\left|\Delta p_j\right|} = 0 \qquad \text{(Eq. 2.4.3)}$$

where n is the number of openings and Δp_j is found for each opening by Eq. (2.4.2).

The ventilation capacity can be calculated as:

$$q_v = ½ \sum_{j=1}^{n} C_{d,j} A_j \left(\frac{\left| ½ C_{p,j} \rho_u v_{ref}^2 - P_i + \frac{\rho_u \Delta T}{T_i} g(H_0 - H_j) \right|}{½ \rho_j} \right)^{½} \text{ (m}^3\text{/s)} \qquad \text{(Eq. 2.4.4)}$$

Example 7

A single zone cubic building with the side length 15 m has to openings in opposite walls. The area of each opening is 0.5 m^2. The bottom opening is located 1m above the floor level and the top opening 13m. The internal temperature are 22 ^oC and the external temperature is t_u = 10 ^oC. The reference wind speed is 4 m/s and the pressure coefficient is $C_{p,l}$ = -0.2 on the leeward side and $C_{p,w}$ = 0.7 on the windward side.

As the opening area and the characteristics are the same for the two openings the neutral plane will be positioned in the height: $H_n = (H_1+H_2)/2$ = 7m and the internal pressure will be an average value of the surface pressure on the windward and the leeward building surface, see Eq. 2.3.6.

The pressure difference across each opening will be the same and for the lower opening on the leeward surface it can be calculated by Eq. (2.4.2):

$$\Delta p = ½ C_p \rho_u v_{ref}^2 - P_i + \frac{\rho_u \Delta T}{T_i} g(H_0 - H)$$

$$\Delta p = ½ \cdot -0.2 \cdot 1.25 \cdot 4^2 - ½\left(\frac{-0.2+0.7}{2}\right)1.25 \cdot 4^2 + \frac{1.25(22-10)}{(273+22)}9.82(7-1) = -1{,}5Pa$$

A negative pressure difference means an outflow of air through the bottom opening, because the wind force is stronger that buoyancy.

The air flow rate through the opening for a discharge coefficient of $C_{d,1}$ = 0,7 becomes:

$$q_v = C_{d,1}A_1\left(\frac{|\Delta p_1|}{½\rho_u}\right)^{½}\frac{\Delta p_1}{|\Delta p_1|} = 0.7 \cdot 0{,}5\left(\frac{|-1.5|}{½ \cdot 1.25}\right)^{½}\frac{-1.5}{|-1.5|} = -0.54\,(\mathrm{m}^3/\mathrm{s})$$

Figure 18 shows the ventilation air flow rate through the building as a function of reference wind speed and temperature difference for wind forces alone and for wind forces assisting and opposing the buoyancy forces, respectively. For opposing wind and buoyancy forces the ventilation flow rate falls to zero when the pressure difference across the opening due to buoyancy is exactly balanced by wind forces.

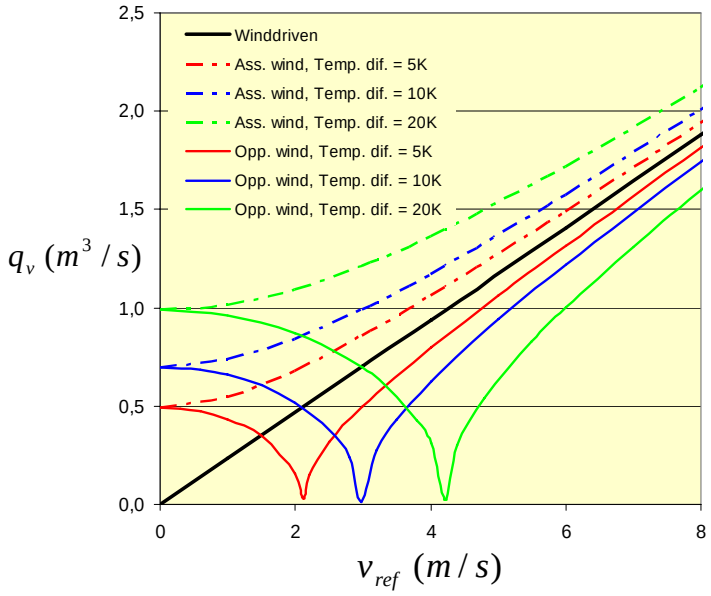

Figure 18. Ventilation flow rate for wind alone and for thermal buoyancy with assisting and opposing wind, respectively, as a function of wind speed and temperature difference.

2.5 Single Zone Ventilation by a combination of thermal buoyancy, wind and fan assistance

The ventilation flow rate due to natural ventilation will change according to outdoor conditions and if they are unfavourable the system might not meet the needs of the building. To establish a more stable ventilation flow and to ensure certain capacity natural ventilation can be assisted by a mechanical fan.

The total pressure difference across an opening will be the sum of pressure differences and can be calculated from Eq. (2.4.2):

$$\Delta p = ½C_p\rho_u v_{ref}^2 - P_i + \frac{\rho_u \Delta T}{T_i}g(H_0 - H) \qquad \text{(Eq. 2.5.1)}$$

In cases, where the supplied or exhausted air flow rate by a fan can be regarded as constant and independent of the natural driving forces, the internal pressure at height, H_o, can be found from the following mass balance by an iterative solution method:

$$\sum_{j=1}^{n} C_{d,j} A_j \rho_j \left(\frac{|\Delta p_j|}{½ \rho_j} \right)^{½} \frac{\Delta p_j}{|\Delta p_j|} + q_m \cdot \rho_i = 0 \qquad \text{(Eq. 2.5.2)}$$

where n is the number of openings, Δp_j is found for each opening by Eq. (2.5.2), and q_m is the air flow rate transported by the fan, which is positive for supplied air and negative for exhausted air.

When the internal pressure is known the air flow rate through the individual opening can be calculated as well as the air flow rate of the zone. Calculations are valid for a constant zone temperature, but will also have an acceptable accuracy in zones with a constant temperature gradient, if the average temperature level is used.

In cases, where the fan is running at a constant rotational speed (rpm) and the pressure conditions outside and inside the building will have an impact on the performance of the fan (the pressure increase by the fan is small compared to the pressure differences created by the natural driving forces), the fan performance curve must be taken into consideration in the mass balance of the system. Eq. 2.5.2 will change to the following:

$$\sum \left(q_{v,j} \frac{\Delta p_j}{|\Delta p_j|} \right) \pm (B_1 + B_2 \Delta p_m + B_3 \Delta p_m^2) = 0 \qquad \text{(Eq. 2.5.3)}$$

where the constants B_1-B_3 is found from the fan performance curve at the specific fan rotational speed. The air flow rate transported by the fan is positive for supplied air and negative for exhausted air. The equation is solved by iteration and when the internal pressure is known the air flow rate through the individual opening can be calculated as well as the air flow rate of the zone.

2.6 Loop equation prediction method for single zone ventilation

Beregningsmodellen formuleres ved at idealisere ventilationssystemet som en række kontrol volumener (fx rum, zoner, kanaler, osv.) forbundet gennem en række komponenter eller strømningsveje (fx vinduer, døre, ventilationskomponenter, armaturer, osv.). Et eksempel på dette er illustreret på Figure 19, hvor et enkelt rum er modelleret med en indtagsåbning (a), et aftræksarmatur i rummet (b), en aftrækskanal (b-c), samt en ventilator og afkasthætte (c). Kontrolvolumenerne i dette tilfælde er rummet, aftrækskanalen, mens strømningskomponenterne er indtag, aftræksarmatur, ventilator og afkasthætte.

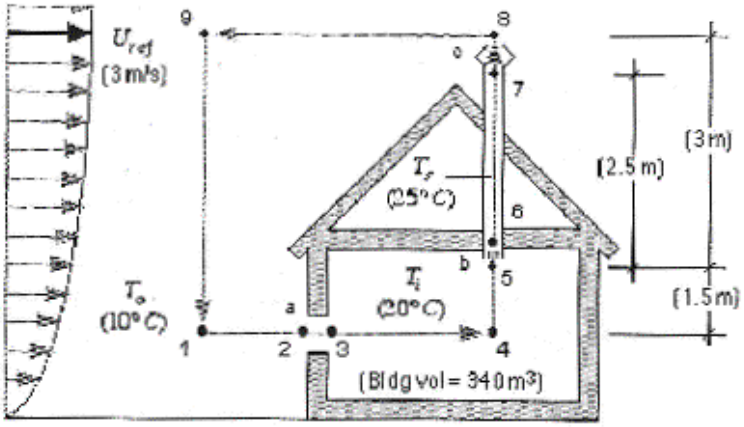

Figure 19. Idealisering af ventilationssystem for en bygning (Axley 2001).

Diskrete knudepunkter identificeres (nummererede punkter i Figure 19) med tilhørende værdier for temperatur og tryk. Temperaturen regnes som konstant i hvert kontrolvolumen og trykket at variere hydrostatisk. Beregningsmodellens bestemmende ligninger opstilles ved at summere udtryk for trykændringer langs en kontinuert strømningsløkke gennem bygningen. En løkke følger en mulig strømningsvej for luften fra knudepunkt til knudepunkt tilbage til det oprindelige knudepunkt. Med Figure 19 som eksempel vil en mulig løkke være at følge strømningsvejen 1-2-3-4-5-6-7-8-9 og tilbage til 1. Summen af trykændringerne langs løkken skal være 0. Ved anvendelse af relationer for drivtryk og tryktab i komponenter kan de bestemmende ligninger for løkkerne opstilles. Med udgangspunkt Figure 19 startende med knudepunkt 1, P_{1o}, og bevægelse i strømningsretningen summeres først trykstigningen på grund af vindtrykket på facaden ved knudepunkt 2, dernæst tryktabet gennem indtaget (vindue), den hydrostatiske trykfald ved højdeændringen fra knudepunkt 4 til 5, tryktabet gennem aftræksarmaturet, osv. For hele løkken fås følgende ligning:

$$\begin{aligned} &\tfrac{1}{2}C_{p,2}\rho_u v_{ref}^2 - \Delta p_a - \rho_i g\Delta H_{45} - \Delta p_b - \Delta p_{bc} - \rho_s g\Delta H_{58} + \Delta p_m \\ &- \Delta p_c - \tfrac{1}{2}C_{p,8}\rho_u v_{ref}^2 + \rho_u g\Delta H_{91} = 0 \end{aligned} \qquad \textit{Eq. 2.6.1}$$

hvor

$$\Delta p_a = \frac{\rho}{2}\left(\frac{q_v}{C_d A}\right)^2 \text{ (tryktab gennem vindue)} \qquad \text{Eq. 2.6.2}$$

$$\Delta p_b = \left(\frac{q_v}{C}\right)^{1/n} \text{ (tryktab gennem aftræksarmatur)} \qquad \text{Eq. 2.6.3}$$

$$\Delta p_{bc} = f\frac{L}{D}\left(\frac{\rho q_v^2}{2A^2}\right)^2 \text{ (tryktab i aftrækskanal)} \qquad \text{Eq. 2.6.4}$$

$$\Delta p_m = a_o\left(\frac{D}{D_o}\right)^2\left(\frac{N}{N_o}\right)^2 + a_1\frac{q_v}{\left(\frac{D}{D_o}\right)}\left(\frac{N}{N_o}\right) + a_2\frac{{q_v}^2}{\left(\frac{D}{D_o}\right)^4}$$ (trykforøgelse i vent.) Eq. 2.6.5

$$\Delta p_c = \alpha q_v + \beta q_v^2$$ (tryktab i afkasthætte) Eq. 2.6.6

Ligning 2.6.1 kan synes noget kompliceret, men indeholder kun:

- En summering af hydrostatiske trykændringer, der resulterer i det termiske drivtryk, Δp_t
- En summering af vintryk på bygningen, der resulterer i det totale vindtryk, Δp_v
- En summering af tryktabet i komponenter og strømningsveje langs løkken, Δp_l

Ligning 2.6.1 kan således skrives:

$$\Delta p_a + p_b + \Delta p_{bc} - \Delta p_{vent} + \Delta p_c = g(-\rho_i \Delta H_{45} - \rho_s \Delta H_{58} + \rho_u \Delta H_{91}) + (C_{p,2} - C_{p,8})½\rho_u v_{ref}^2$$ Eq. 2.6.7

eller på generel form som:

$$\sum \Delta p_{ij} = g\sum \rho_{ij}\Delta H_{ij} + (\Delta C_p)½\rho_u v_{ref}^2$$ Eq. 2.6.8

hvor

- Δp_{ij} er positiv for strømning i løkkens retning (med undtagelse af ventilatorbidraget)
- ΔH_{ij} er positiv for faldende og negativ for stigende højde langs løkken
- ρ_{ij} er luftdensiteten hørende til zonen, hvori højdeændringen foregår
- ΔC_p er summen af trykkoefficienter hvor C_p summeres positivt langs løkken fra omgivelser til vægfladen og negativt fra vægfladen til omgivelserne

3 LITERATURE

M. Santamouris and D. Asimakopoulos.
Passive Cooling of Buildings. James & James Ltd., 1996, ISBN 1 873936 47 8.

Francis Allard.
Natural Ventilation in Buildings – A Design Handbook. James & James Ltd., 1998, ISBN 1 873936 72 9.

Natural Ventilation in Non-Domestic Buildings. Applications Manual AM10:1997, CIBSE. ISBN 0 900953 77 2.

K. Terpager Andersen.
Theoretical Considerations on Natural Ventilation by Thermal Buoyancy. ASHRAE Transactions, Vol. 101, part 2, 1995.
K. Terpager Andersen.
Dimensionering af naturlig ventilation ved termisk opdrift. SBI-Rapport 301, SBI 1998.

Andersen, K.T., Heiselberg, P., Aggerholm, S. Naturlig ventilation i erhvervsbygninger – beregning og dimensionering. *By og Byg Anvisning 202, August 2002, By og Byg. (118s).*

B. H. Shaw and W. Whyte
Air movement through doorways – the influence of temperature and its control by forced airflow. Building Services Engineering, Vol. 42, pp 210-218, 1974.

D. E. Kiel and D. J. Wilson
Combining Door swing pumping with density driven flow. ASHRAE Transactions, Vol. 95, Part 2, pp 590-599, 1989.

J. van der Maas, C. A. Roulet and J. A. Hertig
Some aspects of gravity driven air flow through large apertures in buildings. ASHRAE Transactions, Vol. 95, Part 2, pp 573-583, 1989.

B. A. Majahan
Measurement of interzonal heat and mass transfer by natural convection. Solar Energy, Vol. 38 (6), pp 437-446, 1987.

David Etheridge and Mats Sandberg
Building Ventilation – Theory and measurement. John Wiley & Sons, 1996, ISBN 0 471 96087 X.

P. R. Warren
Ventilation through openings on one wall only. Int. Conf. Heat and Mass Transfer in Buildings, Dubrovnik, Yugoslavia. In: Energy conservation in heating, cooling and ventilating buildings, Vol 1. eds. C. J. Hoogendorn and N. H. Afgar, pp 189-209. Hemisphere, Washington DC, 1977.

P. R. Warren and L. M. Parkins
Single-sided ventilation through open windows. In Conf. Proc. Thermal Performance of the Exterior Envelopes of Buildings, ASHRAE SP 49, pp 209-228, Florida, December 1985.

W. G. Brown and K. R. Solvason
Natural convection through rectangular openings in partitions – vertical partitions. Int. J. Heat & Mass Transfer, Vol. 5, pp 859-868, 1962.

W. de Gids and H. Phaff
Ventilation rates and energy consumption due to open windows – A brief overview of research in the Netherlands. Air Infiltration Review. Vol. 4(1), pp 4-5, 1982.

T. Yamanaka, M. Narasaki and T. Daikoku
Ventilation rate of an enclosure with a single opening exposed to natural wind. The 5th Int. Conf. on IAQ and Climate. Toronto, Canada, July 29 – August 3, pp 479-484, 1990.

H. K. Malinowski
Wind effect on the air movement inside buildings. Proceedings of the third Int. Conf. on Wind on Buildings and Structures, Tokyo, pp125-134, 1971.

J. van der Maas (ed.)
Air flow through large openings in buildings. Annex 20: Air flow patterns within buildings. Subtask 2 Technical Report, IEA-ECBCS, June 1992.

W. G. Brown
Natural convection through rectangular openings in partitions – 2. horizontal partitions. Int. J. Heat & Mass Transfer, Vol. 5, pp 869-878, 1962.

A. Mercer and H. Thompson
An experimental investigation of some further aspects of the buoyancy-driven exchange flow between carbon dioxide and air following a depressurization accident in a magnox reactor, Part 1: The exchange flow in inclined ducts. J. Br. Nucl. Energy Soc., Vol. 14, pp327-334, 1975.

M. Epstein
Buoyancy-driven exchange flow through small opening in horizontal partitions. Journal of Heat Transfer, Vol. 110, pp 885 -893, 1988.

T. A. Conover, R. Kumar and J. S. Kapat
Buoyant pulsating exchange flow through a vent. Journal of Heat Transfer, Vol. 117, pp 641-648, 1995.

J. S. Kohal, S. B. Riffat and L. Shao
An experimental and theoretical investigation of airflow through large horizontal openings. !5th AIVC Conference, Buxton, UK, pp 730-739, 27-30 september, 1994.

D. Blay, J. L. Tuhault and S. Pinard
Heat transfer through a horizontal aperture connecting two non-isothermal rooms. Proceedings of ROOMVENT 98, Vol 2, pp 533 – 538, 1998.

M. Sandberg and C. Blomqvist
A note on air movements through horizontal openings in buildings. Proceedings of ROOMVENT 2002, Copenhagen, Denmark, pp 529 – 533, 2002.

B. A. Majahan and D. D. Hill
Interzonal Natural Convection for Various Aperture Configurations. ASME, Proceedings of Winter Annual Meeting, Anaheim, CA, 1986.

S. B. Dalziel and G. F. Lane-Serff
The Hydraulics of Doorway Exchange Flows. Building and Enviroment, Vol. 26, No. 2, pp. 121-135, 1991.

R. D. Crommelin and E. M. H. Vrins
Ventilation through a Single Opening in a Scale Model. Air Infiltration Review, Vol. 9, No. 3, May 1988.

M. Narasaki, T. Yamanaka and M. Higuchi
Influence of Turbulent Wind on the Ventilation of an Enclosure with a Single Opening. Environmental International, Vol. 15, no. 1-6, pp 627-634, 1989.

Heiselberg, P., Bjørn, E. Impact of Open Windows on Room Air Flow and Thermal Comfort. International Journal of Ventilation, Vol 1, No. 2, pp 91-100, October 2002.

Heiselberg, P., Svidt, K., Nielsen, P.V. Characteristics of airflow from open windows. Building and Environment, 36 (2001), pp 859-869.

Heiselberg, P (ed.) 2002. Principles of Hybrid Ventilation. IEA ECBCS-Annex 35final report. Hybrid Ventilation Centre, Aalborg University, ISSN 1395-7953 R0207. The booklet, technical and case study reports as well as papers from the 1st, 2nd and 4th Hybvent Foum are available for download at http://hybvent.civil.auc.dk.

Seppänen, O. and Fisk, W.J. 2002. Association of Ventilation System Type with SBS Symptoms in Office Workers. Indoor Air, Vol. 12, No. 12, pp 98 – 112.

Rowe, D. 2002. Wilkinson Building The University of Sidney. Case study report in “Principles of Hybrid Ventilation”. Hybrid Ventilation Centre, Aalborg University, ISSN 1395-7953 R0207.

Vik, T.A. 2003. Life cycle cost assessment of natural ventilation systems. Norweigian University of Science and Technology, NTNU, Trondheim. Ph.D. thesis 2003:14, Department of Architectural Design, History and Technology, ISBN 82-471-5561-3.

Van der Aa, A. 2002. Cost of Hybrid Ventilation Systems. Technical report in “Principles of Hybrid Ventilation”. Hybrid Ventilation Centre, Aalborg University, ISSN 1395-7953 R0207

T.S. Larsen, P. Heiselberg and T. Sawachi. Analysis and Design of Single-sided Natural Ventilation. Proceedings of ISHVAC 2003, The 4th International Symposium on Heating, Ventilation and Air-conditioning, October 9-11, Beijing, China, Vol 1., pp 159-163, 2003.

Z. Li, P. Heiselberg and P.V. Nielsen. Characteristics of Buoyancy Driven Single-Sided Natural Ventilation through Horizontal Openings. 2nd International Conference on Built Environment and Public Health, BEPH2004, Shenzhen, China, Dec. 6-8, 2004

Z. Li, P. Heiselberg and P.V.Nielsen. Experimental study of buoyancy driven natural ventilation through single-sided horizontal openings. Under preparation, 2005a.

Z. Li, P. Heiselberg and P.V.Nielsen. Buoyancy driven natural ventilation through a high level horizontal opening and a low level vertical opening. Under preparation, 2005b.

Recent publications in the DCE Lecture Note Series

Heiselberg, P. Modelling of Natural and Hybrid Ventilation. DCE Lecture Notes No. 004, Department of Civil Engineering, Aalborg University, Denmark

Heiselberg, P. Design of Natural and Hybrid Ventilation. DCE Lecture Notes No. 005, Department of Civil Engineering, Aalborg University, Denmark.

ISSN 1901-7286
DCE Lecture Notes No. 004